Long Run Analysis of Crude Oil Portfolios

Roy Cerqueti[1], Viviana Fanelli[2] and Giulia Rotundo[3*]

[1] Department of Economics and Law, University of Macerata,
Via Crescimbeni, 20. I - 62100 Macerata, Italy.
Email: roy.cerqueti@unimc.it
[2] Department of Economics, Management and Business Law, University of Bari
Largo Abbazia Santa Scolatica 53, 70124 Bari, Italy.
Email: viviana.fanelli@uniba.it
[3] Department of Statistical Sciences, Sapienza University of Rome, p.le A. Moro 5,
00185 Roma, Italy.
Email: giulia.rotundo@uniroma1.it

Abstract

This paper deals with the analysis of the long-run behavior of a set of mispricing portfolios generated by three crude oils, where one of the oil is the reference commodity and it is compared to a combination of the other two ones. To this aim, the long-term parameter related to the mispricing portfolio are estimated on empirical data. We pay particular attention to the cases of mispricing portfolios either of stationary type or following a Brownian motion: the former situation is associated to replication portfolios of a reference commodity; the latter one allows to implement forecasts. The theoretical setting is validated through empirical data on WTI, Brent and Dubai oils.

Keywords: Commodities portfolio, long-term memory, forecast, crude oils.

1 Introduction

Among the characterizing features of a time series, a relevant role is played by the so-called *persistence* or *long-term memory property*. Such aspect is related to the autocorrelation of the time series, and reflects the behavior of the process on the long-run. Hurst (1951) has been the pioneer of the formalization of the concept of long-term memory property for a hydrological time series.

The persistence property of a time series has a relevant informative content in many applied contexts. This paper deals with one of the most prominent one. In fact, we consider the series of deviation of the price of a portfolio of commodities from a reference commodity. In so doing, we explore the long-term memory properties of a so-called *mispricing portfolio* of commodities. The selected commodities are crude oils. Yet, the persistence properties of a mispricing portfolio of crude oils explains the replicability of the reference oil price dynamics through the non reference oils. This is of paramount importance in many respects, like hedging and assessing statistical arbitrage effects.

In general, the exploration of the long-run behavior of a time series brings key information on

---

*Corresponding author.

if and how the related phenomenon can be predicted (see e.g.: Corazza and Malliaris (2002); Cajueiro and Tabak (2004); Kyaw et al. (2006); J.P. and Sella (2008); Potgieter (2009)). Furthermore, in the field of finance, the existence of long-term memory associated with slow decay of autocorrelation functions in asset returns indicate the existence of exploitable market inefficiencies as suggested by Baillie (1996).

We feel close to the mentioned papers for our purpose of gaining insights on the properties on the long-run of an aggregation of crude oils prices by discussing the predictability of the mispricing portfolio.

We choose to analyse the crude oil markets because their dynamics play a central role in the worldwide economy since oil price movements substantially affect the most macroeconomic activity, especially after the 1970s crises (see Barsky and Kilian (2004), Kilian (2009), Ferraro et al. (2015)). A great deal of recent literature discusses the efficiency of crude oil markets (see, for example, Ortiz-Cruz et al. (2012)) and research focuses on the dynamics of the three major crude oil prices, that is WTI, Brent and Dubai oils (see, for example, Kristoufek and Vosvrda (2014)), with a particular interest in the empirical evidence of long-run dependence phenomena for prices. In this respect, Alvarez-Ramirez et al. (2002) and Serletis and Andreadis (2004) show that long-run memory mechanism affects the crude oil price evolution, but Tabak and Cajueiro (2007) suggest that the crude oil market has exhibited a temporal movement towards efficiency. More recently, Alvarez-Ramirez et al. (2008) examine the empirical evidence of long-run autocorrelations in crude oil markets towards efficiencies and they analyze also short-term autocorrelations dynamics. Wang and Liu (2010) extend the existing literature by testing for the efficiency of WTI crude oil market through observing the dynamics of the local long-term parameter. They employ the method of rolling window and find that the small fluctuations of WTI crude oil market are persistent; however, the large fluctuations have high instability, both in the short- and long-terms.

We are quite different from the quoted papers. Indeed, as already preannounced above, we here do not focus on the single commodities. Rather than this, we consider a suitable aggregation of three crude oil prices, quoted in different markets: WTI, Brent and Dubai. In particular, WTI is the reference commodity while Brent and Dubai are combined together to create a replicating portfolio of WTI. The price of the mispricing portfolio is given by the difference between the price of the WTI and the one of the replicating portfolio of Brent and Dubai. Indeed it is natural thinking that three assets, having same specific features and supply and demand with the same characteristics, have prices that are influenced by market rumors with the same magnitude and incremental direction. Moreover, WTI, Brent and Dubai are commonly considered as crude oil benchmarks and the comparison among them is a relevant theme in the empirical analysis of crude oil markets (see, for example, **?**, **?**, **?** and **?**).

It is worth noting that the use of a price combination instead of a single price has a further financial meaning, beyond the aspects listed above. In fact, a price combination is a relative value, and, if chosen in an appropriate way, it can be statistically independent of market-wide risks and influenced only by commodity specific aspects. This statement is at the basis of traditional asset pricing models such as CAPM (Capital Asset Pricing Model) and APT (Arbitrage Pricing Theory). The point is that the noise or stochastic component in asset returns is common to many assets in the market, so an appropriate combination of asset prices can eliminate the effect of market-wide risk factors. Consequently, combination dynamics are affected only by asset specific component dynamics that are potentially more predictable (see Vidyamurthy (2004)).

2

The long-term memory property is assessed through the estimation from empirical time series of a parameter, denoted usually as H. Here, in order to face the problem, we propose a statistical-based analysis of a selection of empirical portfolios obtained by the available commodities data, and discuss the long-run properties of them through the estimation of H.

We here specifically explore two remarkable cases of long-run behaviors: the situation of stationary mispricing portfolios and the one associated to mispricing portfolios evolving in accord to a Brownian motion (Bm). The former case relies to how one can replicate the WTI through a portfolio of Brent and Dubai. In this respect, we point out that if the three series are I(1), then the existence of a stationary combination of them suggests that the three oils are cointegrated; the latter case allows to implement forecast on the future evolution of the price of the mispricing portfolio.

The analysis takes into consideration several aspects of the problem. First, the presence of structural breaks in the dynamics of the crude oils; second, the dependence of the long-run properties of the mispricing portfolios on the considered time-window. In this respect, we have implemented the analysis over different time length frameworks and discussed the related results. Third, the forecast of the mispricing portfolio evolution in the case of Bm. Obtained results are interesting. A good amount of mispricing portfolios doesn't reject the hypothesis of either stationarity or of Bm. We have also shown their presence and spread on the length of the time windows, through a separate measurement. Moreover, there is evidence that short-term (5 days) forecast of mispricing portfolio prices following a Bm time window are more accurate when they are still proxied through Bm instead of using already the empirical H of the next time window.

The rest of the paper is organized as follows: Section 2 contains the conceptualization of the mispricing portfolio; Section 3 is devoted to the description of the data; Section 4 illustrates in details the employed methodological tools; Section 5 presents and discusses the outcomes of the analysis; last Section offers some conclusive remarks. The Appendix adds insights on the choice of the algorithm for the numerical estimate of H.

2   The definition of mispricing portfolios

Let $(\Omega, F, (F_t)_{t\geq 0}, P)$ be a filtered probability space over an infinite horizon $[0, \infty)$, satisfying the usual conditions. P is the statistical probability measure.

The commodity market we deal with is populated by $J > 0$ commodities. The price at time $t > 0$ of the j-th commodity is C_t^j, for each $j = 1, 2, \ldots, J$.

We also consider a further *reference commodity* in the market, whose price at time t is denoted by T_t. The reference commodity plays the role of a target commodity for the investor. The target asset can be replicated through a portfolio of the J no-reference commodity of the market, that represents a synthetic asset, whose value at time t is indicated by Z_t.

Then the following statistical fair-price relationship holds:

$$E[T_t|\mathcal{F}_s] = E[Z_t|\mathcal{F}_s], \quad 0 \leq s \leq t, \tag{1}$$

where $E[\cdot|\mathcal{F}_s]$ is the expected value under the objective probability measure $\mathbb{P}$ conditional to the information available at time s, $\mathcal{F}_s$.

It could occur that the long-run relationship (1) fails in the short-term, due to a mispricing of the considered commodities, so that we can focus on deviations $T_t - Z_t$, $t \geq 0$. Specifically,

consider a long-short portfolio, such that a long (short) position on a target commodity and a short (long) position on a synthetic asset are assumed.

Formally, if we denote as M_t the price of the long-short portfolio at time t, we have:

$$M_t = T_t - Z_t = T_t - \sum_{j=1}^{J} \beta_j C_t^j, \qquad (2)$$

where Z_t is the price of the synthetic asset at time t and $(\beta_1, \beta_2, \ldots, \beta_J)$ is its replication portfolio.

By definition, the long-short portfolio can be also viewed as a mispricing portfolio. In fact, deviations between the target commodity price and the replication portfolio value represent statistical mispricings. As the values of $\beta_1, \beta_2, \ldots, \beta_J$ change, mispricing portfolio change as well. Thus, $\beta_1, \beta_2, \ldots, \beta_J$ identify a class of portfolios (see Section 4 for the detailed selection of mispricing portfolios explored in this paper).

3 Data

Many types of crude oils are selected around the word. The market value of an individual crude oil reflects its intrinsic quality characteristics, and, in particular, the density and sulfur content. The buyers use some benchmarks in order to choose, among different crude oils, the more desirable one in terms of quality and location and in function of the final use and destination. Benchmarks are traded and quoted in public view and relatively frequently, so that they are visible and identifiable. Furthermore, benchmarks are important because they are used as reference for pricing financial and physical assets, regionally and globally.

Among several benchmarks, we choose the three primary ones, because the price of most crude oils are pegged to them:

- Brent refers to oil from four different fields in the North Sea: Brent, Forties, Oseberg and Ekofisk. It is light and sweet and it is easy to transport. Brent is traded on the Intercontinental Exchange (ICE) and it was launched in July, 1989. It is the main European benchmark.

- West Texas Intermediate, or WTI, refers to oil extracted from wells in the United States and sent via pipeline to Cushing, Oklahoma. It is very light and very sweet, but it is also expensive to transport. WTI, traded on the New York Mercantile Exchange (Nymex), was launched in March, 1983, and it is now the most liquid contract and the main benchmark in the United States.

- Dubai/Oman refers to oil from Dubai, Oman or Abu Dhabi. It is heavier and sourer than Brent and WTI and it is quoted by Platt's. It is the main reference for Persian Gulf oil delivered to the Asian market.

In this paper, we use daily one-month futures prices and our data set spans from 01/01/2007 to 04/25/2017. Each futures contract is traded until the close of business on the third business day prior the 25th calendar day of the month presiding the delivery month and it is assumed that the investor will roll over the front month pair contracts the first day of the trading month. In our case, WTI crude oil is the reference commodity and Brent and Dubai crude oils are held in the replicating portfolio. Hence, $J = 2$ in equation (2).

Time interval $[0, +\infty)$ is conveniently discretized. In details, we consider an increasing sequence of trading dates $(t_i)_{i \in \mathbb{N}}$.

Z_{t_i} denotes the price at time t_i of the portfolio consisting of the commodities Brent and Dubai, while T_{t_i} is the target price associated to the reference commodity WTI crude oil. Hence, the price of the mispricing portfolio is then obtained according to the following relationship:

$$M_{t_i} = T_{t_i} - Z_{t_i} = T_{t_i} - \sum_{j=1}^{2} \beta_j C_{t_i}^{j}, \tag{3}$$

where β_1 and β_2 are the weights generating the portfolio replicating the synthetic asset, while $C_{t_i}^{1}$ is the price of the Brent oil and $C_{t_i}^{2}$ is the price of the Dubai oil at time t_i.

4   Methodology

This section contains all the methodological procedures implemented for the analysis of the mispricing portfolios.

4.1   Detection of the structural breaks

In this section, we investigate the long-term equilibrium among the considered crude oils, WTI, Brent and Dubai. Specifically, we here deal with the assessment of the cointegration among the series.

Roughly speaking, we say that some time series are cointegrated when data of single time series are non-stationary purely due to unit roots (integrated once, denoted I(1)), but there exists a linear combination of them with nonnull coefficients which is stationary (denoted I(0)).

We are here interested in cointegration because it assumes coefficient stability in the long-run equilibrium among oil prices. However, it is recognized that such stability may not reflect empirical data, particularly large sample data. In the literature, some authors consider the possibility of cointegration even if there are structural breaks in time series, such as Gregory and Hansen (1996).

Thus, cointegration represents a mean to assess the presence of structural breaks for a stationary combination of the series and to localize them.

The stationary linear combination obtained by exploring cointegration can be written by stating the existence of $\beta_1, \beta_2 \in \mathbb{R}$ such that:

$$T_t = \beta_1 C_t^1 + \beta_2 C_t^2, \quad t \geq 0. \tag{4}$$

Equation (4) means that we can find a portfolio consisting of Brent and Dubai that replicates the value of WTI at any time.

Coefficients α_1 and α_2 are estimated by applying the cointegration regression. In particular, we regress a set of historical Brent and Dubai prices over historical WTI prices, such that

$$(\alpha_1, \alpha_2) = \arg \min \sum_t \left(T_t - \alpha_1 C_t^1 - \alpha_2 C_t^2 \right)^2 . \tag{5}$$

There is evidence for a cointegrating relationship if: *(a)* we apply the Augmented Dickey-Fuller test and the unit-root hypothesis is not rejected for the individual series $(T_t)_{t \geq 0}$, $(C_t^1)_{t \geq 0}$ and $(C_t^1)_{t \geq 0}$, namely they are I(1), and *(b)* we apply the Augmented Dickey-Fuller

test and the unit-root hypothesis is rejected for the residuals from the regression, that is they are stationary, I(0).

By using observations 01/01/2007-04/25/2017 the cointegration analysis gives the following results:

1. WTI, Brent and Dubai time series are I(1);

2. The regression coefficients are:

	estimate	std. error	t-ratio	p-value
const	6.05012	0.423978	14.27	1.37e-044
α_1	0.737202	0.0634526	11.62	1.76e-030
α_2	0.126665	0.0637457	1.987	0.0470

3. The residuals from regression are I(0).

To detect the structural breaks, the Quandt likelihood ratio (QLR) test of Stock and Watson (2003) is applied. In particular, we verify in this way that coefficients α_1 and α_2 in equation (4) are stable in the long period. The QLR F-statistics test the hypothesis that the intercept and coefficients in formula (4) are constant against the alternative of break in the central 70% of the sample. This test identifies the date of the structural break over a considered time period.

Figure 1 helps us to understand the dynamics and potential relationships between crude oils in order to recognize structural break dates.

The QLR test identifies the most significative break in a given time period and since we want to investigate if there are more than one break in the series, we implement an iterative procedure for multiple breaks in subsamples of the original dataset. In each step of the procedure we verify the cointegration for the considered time series and we perform the QLR test in order to find a break point Q_1 belonging to the subsample under investigation.

4.2 Assessment of the long-term memory of the mispricing portfolios and estimate of H

Many studies in the field of econophysics have also examined properties and phenomena of financial time series through interdisciplinary studies and found presence of long memory in the time series and notable deviations from random walk.

The long-term memory, or long-range persistence, refers to the slow decay of the autocorrelation function, as the time delay increases. After a pioneering paper of Hurst (1951), which is based on estimating range of swings of the variable over time, different mathematical definitions of long-term memory have been used for different contexts and purposes, for instance relating the long-term parameter H to parameters describing fractionally integrated processes, and self-similar processes Ausloos (2002); Bardet et al. (2003).

In general, a great amount of literature deals with several techniques that can be used to estimate H. Among the others, Ausloos (2002); Bardet et al. (2003); Kirichenko et al. (2011) compare some of them. In this paper, the subroutine $wfbmesti$ from the $MATLAB$ package has been selected in order to estimate the parameter H associated to the time series $(M_t)_{t \geq 0}$ Bardet et al. (2003); Istas and Lang (1997); online manual (2006). The estimate uses a generalization of the quadratic variation. Details on the algorithm implemented and the rationale of the choice are described in the Appendix, as well as the values of the mean value m of H estimated over 100000 simulation and the related standard deviation σ, both

for the uncorrelated and the Bm case.

The bounds $m \pm \sigma$ are used in the next data analysis to fix the confidence intervals: the hypothesis of uncorrelated data is not rejected if $H \in (-\sigma, +\sigma)$; the hypothesis of Bm is not rejected if $H \in (0.5 - \sigma, 0.5 + \sigma)$. The values of m and σ are reported in the Appendix, too.

Definition (3) explains, in particular, that the selection of the couple (β_1, β_2) affects the value of H. In our experiments we fix a range for β_1 equal to $[-2, 2]$. In so doing, we include a wide possibility of short selling. Furthermore, to deal with portfolios, we set $\beta_2 = 1 - \beta_1$. In order to implement extensive analysis and to avoid computational complexity, we limit our attention to a discretization of the range and obtain eleven portfolios, with $\beta_1 = \{-2.00, -1.40, -1.20, -1.00, -.60, -0.20, 0.20, 0.60, 1.00, 1.40, 2.00\}$. Such a discretization choice is reasonable, since it includes a wide perspective on the different natures of the mispricing portfolios in terms of how it is invested in the single crude oils, but still allows to have a readable figure.

The mispricing process has been analyzed in terms of its moving windows with length Δ_l, for each $l = 1, \cdots, 10$. However, not all the windows with the same length have been considered: we start from the very first day t_0, and the next time windows examined starts at $t_0 + 5$. In general, the n-th time windows examined starts at $t_0 + 5n$. This sliding of 5 days ahead corresponds to a working week, it brings the benefit to improve the computational time compared to a slide of 1 day only, and ensures a change of H smoother than on non overlapping time window. To enter the details of the procedure, let us fix a length Δ_l, and denote by $(\bar{\beta}_1, \bar{t})$ the time window starting at time $\bar{t}$, ending in $\bar{t} + \Delta_l$ where portfolio with $\beta_1 = \bar{\beta}_1$ is analyzed. [1]

In order to perform a comprehensive analysis, for each selected length Δ_l, we build two different sets of figure as follows:

- First setting (uncorrelation)

  1. for each rectangle (β_1, t) we estimate H on the time series of the mispricing calculated with the selected β_1, starting at time t, and ending at time $t + \Delta l$;

  2. if the hypothesis of uncorrelation cannot be rejected, we draw a black rectangle starting at the x-coordinate at $t/5$, and at the y-coordinate at β_1, with a width of 1 and height of 0.5.

- Second setting (Brownian motion): the item 1 is as above, the item 2 is substituted by

  2'. if the hypothesis of Bm cannot be rejected, we draw a black rectangle starting at the x-coordinate at $t/5$, and at the y-coordinate at β_1, with a width of 1 and height of 0.5.

In order to understand eventual differences in cointegration, we decided to split our series into intra-break time sub-series not showing structural breaks. Therefore, for each Δ_l, we put in evidence the analysis on the following 5 different segments:

I: 2007-07-27 - 2011-01-06

---

[1]Clearly, the series identified by (β_1, t) depends also on Δ_l, but we omit a reference to such a dependence for the sake of notation.

II: 2011-01-06 - 2013-04-08

III: 2013-04-08 - 2014-02-14

IV: 2014-02-14 - 2015-08-27

V: 2015-08-27 - 2017-04-10 (end of the downloaded data at the time of the analysis)

4.3 Model risk assessment

To provide a better analysis of the stability of the long-term parameter H across adjacent time windows, we also have dealt with a model risk assessment. Indeed, in spite of small fluctuations in data and of the presence of confidence intervals, working with real data implied the unlucky occurrence of a change of the data properties, which affects the validity of the applied model.

Even if only a *a posteriori* analysis can validate the model, we can perform a scenario analysis to understand the frequency with which the hypotheses hold. We perform two different tests. First, for any fixed time length, given a time window where the hypothesis $H = 0$ ($H = 0.5$) holds we estimate the probability distribution of the values of H in the next time window, with the same length. Second, we change perspective and examine the implication of the change of H in the goodness of the forecast following Bm windows (expressed through the MSE) detailed in the next section. We split the analysis into the intra-break zones in order to check similarities and differences.

4.4 Analysis of the forecast

The detection the time windows where the mispricing can be considered as following a Bm opens the way to a practical question. To illustrate it, let us fix a length Δ_l, keep the selected β_1 fixed, and focus on the time parameter. As soon as a couple (β_1, t) gives rise to a black square in the second setting, it means that the Bm hypothesis was not rejected on the portfolio of mispricing calculated with the selected β_1 and on the time window starting in t and ending in $t_1 = t + \Delta_l$. Let us name w_t such a series. Of course, the time window starting at $t_1 + 1$ is going to be characterized by a different value of H, not necessarily being in the Bm range.

Suppose to deal with the forecast in the 5 days since $t_1 + 1$ till $t_1 + 5$. Is the Bm forecast on this 5 days still performing better than the fBm one? In other terms, how many times the next 5 days (following a Bm time window, and keeping the same β_1) are still well suitable for the Bm model, at least more than the fBm one?
In order to tackle the problem we split the analysis depending on the length Δ_l of the windows used for the calculus of the H, and show the result through a graphical representation and through tables. For the graphical representation: for each length in Δ_l we build a figure such that:

1. for each rectangle satisfying the items 1 and 2'

   - let z_0 be the last value of the mispricing portfolio (the value in t_1);
   - 100 samples of a standard Bm time series $(x_t)_{t=1,\ldots,5}$ are generated and a rescaling transformation is applied so to guarantee that the width of the increments of the

forecast, namely $(z_t)_{t=1,\dots,5}$, equals the width of the increments of the time series $(w_t)_{t=1,\dots,5}$ [2]

- the forecast error MSE_{Bm} is calculated as MSE of z_t w.r.t. w_t

- knowing the value of H on the time window identified by the next rectangle (that means with the same value of β_1, but starting in $t+5$, so including the 5 days indicated for the forecast), 100 samples of a fBm time series $(x_t^f)_{t=1,\dots,5}$ are generated and a rescaling transformation is applied so to guarantee that the width of the increments of the forecast (z_t^f) equals the width of the increments of the time series w_t

- the forecast error MSE_{fBm} is calculated as MSE of z_t^f w.r.t. w_t

2. if $MSE_{fBm} > MSE_{Bm}$, so if the fBm forecast performs better than a Bm one, then a black square is drawn in the same position;

3. a red square is drawn otherwise.

The rationale of this approach is that when the Bm time series $(w_t)_{t=1,\dots,5}$ finishes, we cannot know at once the value of H on the series slided 5 days ahead. Therefore, *a priori* we can take the decision to perform the forecast supposing that the next 5 days still obey a Bm motion. But *a posteriori* we find that the value of H may have changed, and the fBm becomes the right theoretical hypothesis for the forecast. Is the change really relevant to the MSE?

Once more, we split the analysis into the intra-break zones in order to check similarities and differences.

5   Results and discussion

As already said above, the procedure of assessment of the structural breaks has given the following dates:

- By using observations 07/01/2007-07/24/2017 the break occurs at date 06/01/2011;

- By using observations 07/01/2007-06/01/2011 the break occurs at date 07/27/2007;

- By using observations 06/01/2011-07/24/2017 the break occurs at date 04/08/2013;

- By using observations 04/08/2013-07/24/2017 the break occurs at date 02/14/2014;

- By using observations 02/14/2014-07/24/2017 the break occurs at date 08/27/2015.

We can give some explanations about the obtained structural breaks by referring to macroeconomic and geopolitical events which have affected the behaviour of crude oil prices and, in particular, the relationship between WTI and Brent.

In the first half of 2007, until the first break, WTI price was mainly higher than the price of the other two crude oils. After the break, the gap switched and in particular Brent

---

[2]Practically:

(a) The mean m_x of the increments of the forecast x is calculated.

(b) The mean m_w of the increments of the Bm series w is calculated.

(c) The forecast z_t is given by $z_t = z_0 + \frac{m_w}{m_x} \sum_{i=1}^{t}(x_t - x_{t-1})$, for $t = 1, \dots 5$.

price went above the WTI price, in which the peak came in February 2009 with an average gap of 4.23$/barrel. Some macroeconomic changes affected this spread, such as the changes in Euro/USD. This evidence caused more volatility in crude oil markets that is reflected in a wider spread oscillation.

The structural break in 2011 can be attributed to several important events that impacted crude oils prices. WTI price was pushed down by the storage and pipeline capacity constraints at Cushing, Oklahoma, an oil-trade hub and the delivery location for NYMEX crude oil futures contracts. Furthermore, on one hand, the Brent price increased as consequence of the Tunisian revolution in December 2010, the raised weight of Brent and decreased weight of WTI in Standard and Poor's S&P GSCI commodity index in January 2011, the Libyan crisis in February 2011, and the Fukushima-Daiichi nuclear disaster in Japan in March 2011, on the other hand, the increase of U.S. production caused a depreciation of the WTI. Dubai price is strongly correlated to Brent price, in fact, although Dubai is the main Asia crude marker, Brent remains a default alternative in Asia.

In the first half of 2013 the WTI strengthened with respect to Brent due to different factors. In the United States several new crude transportation projects, such as pipelines and crude-by-rail terminals, facilitated the transportation of crude oil in U.S. Midcontinent, particularly around Cushing, Oklahoma. Furthermore, refineries run at some of the highest levels on record since 2007. Consequently, WTI price increased until the summer of 2013. Due to the WTI similar quality to Brent, the expanded production of WTI and the easier transportation, some refineries all over the world replaced Brent and Brent-like crude imports, putting downward pressure on Brent prices.

In 2014 there was a structural break maybe due to the spread between WTI and Brent and WTI and Dubai crude oil that began to narrow, even if it remained negative. It was due to the fact that additional transportation infrastructure came online and costs to move WTI crude oil from Cushing to the Gulf Coast diminished. Furthermore, in the United States petroleum products were consumed in 2014 over 2013 levels, which also contributed to greater support for the WTI market than the other crude oil markets. Therefore, the importation of Brent reduced in the United States, but the Libyan supply increased into the Atlantic basin market, so that Brent price was pushed down.

In 2015 lower crude oil prices reflected the continued excess of crude oil supply over global demand. As a result, global crude oil and other liquids inventories increased continuously through the year. The spread between WTI and Brent and WTI and Dubai crude oil continued to narrow. According to data from the Joint Organizations Data Initiative (JODI) the Dubai production in Saudi Arabia and Iraq increased, and the internal demand of crude oil in Saudi Arabia was seasonally low. In these circumstances Dubai price decreased and crude oil was exported from Iraq and Saudi Arabia.

Figures 2-11 show the result of the test of the hypothesis of uncorrelated motion, while Figures 12-21 show the results of the test of the hypothesis of Bm. The vertical bars point out the times of the structural breaks. We remark that since the range has already been fixed equal to $[-2, 2]$, here we are going to perform the analysis on the values $\beta_1 = \{-2, -1.40, -1.20, -1.00, -.60, -0.20, 0.20, 0.60, 1.00, 1.40, 2.00\}$. The 5-days sliding roughly corresponds to a week shift, and allows to keep at a reasonable level the computational time.

Looking through the figures, we remark that, as soon as the time length increases, the distribution of the uncorrelated time window shrinks and gathers. Similar comments hold for the Bm hypothesis testing. In this case, it is worth noticing that in the last 2 intra-break zones the Bm hypothesis is not holding any more for time windows longer than 150; for

time length 250 it is holding only for some values of the parameters in the first intra-break zone.

A first analysis of the percentage of the number of the black squares over all the possible squares is given in Table 5. However, this is just a first rough calculus: the way in which the windows are distributed is relevant for the application of models. In fact, a quick alternation of rejection/not rejection of hypothesis implies the need of a frequent test of the hypothesis. In order to understand the distribution of the black rectangles from a fractal perspective, we calculate the Haussdorf dimension Ausloos (2002) of the Figures 2-11 and 12-21. Figures 22-23 show the results. Table 5 reports the numerical values.

The analysis of the Haussdorf dimension is different from the mere analysis of the percentages, because it considers the spread of the black boxes over the plane. Remarkably, there is a nearly monotonic decrease of the percentage with the length of the time series, with remarkable exceptions. The Haussdorf exponent is not decreasing as well in time zones II, III and V for the uncorrelated hypothesis testing. This means that in spite of the decrease of the number of the time uncorrelated windows, their spread increases in the II, III and V zones as soon as small time windows are gathered to have a longer one. This implies that for longer time series there are less uncorrelated windows, but still distant each from the other. The high peak corresponding to the intra-break time zone V at length 125 shows the maximal dispersion. Further remarks can be added to the behavior in zone I. The increase of the percentage of uncorrelated windows from length 50 to length 75 corresponds to a small reduction of the Haussdorf dimension: this means that the uncorrelated windows tend to cluster together, reducing the spread. The increase of the percentage for the length 100 corresponds to an increase of the Haussdorf dimension: so both the number and the spread of the uncorrelated time windows increase.

In the context of model risk assessment, Figure 24 shows the conditional probabilities to measure H equal to the value reported on each of the x-axis, knowing that in the previous window H was in the confidence interval of 0. The Jarque-Bera test of normality was done on such empirical distribution. The figures in black don't reject the Gaussian hypothesis, the figures in white do reject it. The rows report the measurement for the corresponding intra-break time window. The columns divide the measurement depending on the length of the time series where H has been estimated. From a visual inspection, it is clear that none of the histograms could have been generated by a uniform random distribution. It may be seen that most of the Gaussian distribution appear in the III intra-structural break zone. Therefore, this is the zone with the highest level of uncorrelation.

The procedure for drawing Figure 24 is as follows:

1. for each time zone $\mathcal{I}_b$: intra-break, plus on the entire daset ($\mathcal{I} = (I, II, III, IV, V, all)$),

2. for each time window length $u_l \in \{25, 50, 75, 100, 125, 150, 175, 200, 225, 250\}$,

3. for all the (β_1, t) square where the hypothesis of uncorrelation cannot be rejected,

   - store sequentially in the vector v the value of H estimated on the subsequent window $(\beta_1, t + 5)$.

4. at the end of the above procedure there are 6×10 vectors v.

5. show in the subplot positioned in $\mathcal{I}_b$ with time window of length u_l the histogram of v, where the bars are black if the hypothesis of Gaussian distribution cannot be rejected; white otherwise.

time zone	I	II	III	IV	V	all
H=0						
25	0.5627	0.6109	0.6364	0.6375	0.6011	0.5945
50	0.5038	0.5300	0.6263	0.6122	0.5743	0.5435
75	0.5140	0.4669	0.5414	0.6064	0.5059	0.5144
100	0.5368	0.4746	0.4990	0.6904	0.5027	0.5325
125	0.4931	0.4052	0.4889	0.6697	0.4182	0.4822
150	0.5013	0.3529	0.4303	0.6812	0.3529	0.4598
175	0.4896	0.3421	0.4424	0.6709	0.2930	0.4425
200	0.4728	0.3297	0.4545	0.6490	0.2652	0.4272
225	0.4718	0.3552	0.5434	0.6709	0.2684	0.4434
250	0.4266	0.3390	0.5576	0.5869	0.2321	0.4060
$H = 0.5$						
25	0.3875	0.4222	0.4283	0.3257	0.3230	0.3746
50	0.2275	0.2535	0.2384	0.1623	0.0984	0.2018
75	0.1508	0.1441	0.1677	0.0771	0.0225	0.1170
100	0.1178	0.0670	0.1495	0.0173	0.0043	0.0735
125	0.0808	0.0277	0.1131	0.0000	0.0011	0.0453
150	0.0589	0.0123	0.0485	0.0000	0.0000	0.0280
175	0.0564	0.0046	0.0364	0.0000	0.0000	0.0243
200	0.0538	0.0008	0.0182	0.0000	0.0000	0.0208
225	0.0493	0.0000	0.0040	0.0000	0.0000	0.0178
250	0.0452	0.0000	0.0000	0.0000	0.0000	0.0160

Table 1: Percentages of the black rectangles over the different intrabreak zones. The time zones are listed in order of their appearance. The last column reports the result on all the zones as they were one figure, only.

time zone	I	II	III	IV	V	all
$H = 0$						
25	1.2826	1.4087	1.4278	1.3219	1.3380	1.3007
50	1.2552	1.3673	1.4219	1.3075	1.3061	1.2813
75	1.2491	1.3352	1.3768	1.3034	1.2733	1.2661
100	1.2561	1.3360	1.3555	1.3254	1.2714	1.2686
125	1.2359	1.3078	1.3535	1.3227	1.4751	1.2515
150	1.2331	1.2657	1.3295	1.3313	1.4253	1.2417
175	1.2289	1.2441	1.3309	1.3285	1.3710	1.2323
200	1.2242	1.2332	1.3372	1.3164	1.3506	1.2249
225	1.2227	1.2457	1.3785	1.3210	1.3455	1.2274
250	1.2038	1.2337	1.3808	1.2870	1.2961	1.2138
$H = 0.5$						
25	1.2148	1.3302	1.3270	1.1757	1.2087	1.2313
50	1.0911	1.1938	1.1630	1.0728	0.9130	1.1110
75	1.0005	1.0765	1.0673	0.8850	0.5667	1.0136
100	0.9477	0.8641	1.0164	0.5966	0.2889	0.9255
125	0.8597	0.6662	0.9408	NaN	0.0000	0.8223
150	0.8002	0.4924	0.6671	NaN	NaN	0.7399
175	0.7616	0.4370	0.6968	NaN	NaN	0.6967
200	0.8250	0.0000	0.5034	NaN	NaN	0.6687
225	0.8089	NaN	0.1786	NaN	NaN	0.6529
250	0.8320	NaN	NaN	NaN	NaN	0.7282

Table 2: Haussdorf dimension. The time zones are listed in order of their appearance. The last column reports the result on all the zones as they were one figure, only. The NaN values correspond to the windows with a too low density of black zones.

	I	II	III	IV	V	all
25	0.06(0.25)	0.07(0.24)	0.08(0.25)	0.03(0.24)	0.04(0.25)	0.06(0.25)
50	0.03(0.16)	0.05(0.15)	0.07(0.14)	0.03(0.14)	-0.00(0.14)	0.03(0.15)
75	0.01(0.13)	0.05(0.12)	0.06(0.11)	0.01(0.10)	0.01(0.12)	0.02(0.12)
100	0.01(0.11)	0.06(0.10)	0.05(0.09)	0.02(0.10)	0.01(0.10)	0.03(0.10)
125	0.01(0.09)	0.06(0.09)	0.04(0.07)	0.02(0.08)	0.01(0.09)	0.03(0.09)
150	0.01(0.08)	0.03(0.09)	0.03(0.07)	0.03(0.07)	0.00(0.09)	0.02(0.08)
175	0.02(0.07)	0.02(0.08)	0.03(0.07)	0.04(0.07)	0.01(0.08)	0.02(0.07)
200	0.02(0.06)	0.02(0.07)	0.03(0.06)	0.04(0.06)	0.01(0.08)	0.02(0.06)
225	0.02(0.06)	0.03(0.06)	0.02(0.06)	0.05(0.05)	-0.01(0.07)	0.02(0.06)
250	0.02(0.06)	0.02(0.06)	0.01(0.05)	0.05(0.05)	-0.02(0.06)	0.02(0.06)

Table 3: Table corresponding to Figure 24, Mean and standard deviation (among parentheses) of each of the subplot in the figure.

	I	II	III	IV	V	all
25	0.35(0.23)	0.36(0.22)	0.35(0.26)	0.32(0.26)	0.27(0.24)	0.34(0.24)
50	0.39(0.14)	0.39(0.12)	0.40(0.13)	0.40(0.13)	0.34(0.11)	0.39(0.13)
75	0.42(0.10)	0.38(0.07)	0.41(0.08)	0.39(0.07)	0.35(0.05)	0.41(0.09)
100	0.44(0.09)	0.39(0.06)	0.42(0.05)	0.30(0.13)	0.32(0.05)	0.42(0.08)
125	0.46(0.08)	0.39(0.07)	0.41(0.04)	0.00(0.00)	0.00(0.00)	0.44(0.08)
150	0.47(0.07)	0.39(0.08)	0.43(0.05)	0.00(0.00)	0.00(0.00)	0.46(0.07)
175	0.48(0.06)	0.38(0.03)	0.43(0.05)	0.00(0.00)	0.00(0.00)	0.47(0.06)
200	0.47(0.05)	0.00(0.00)	0.39(0.04)	0.00(0.00)	0.00(0.00)	0.47(0.06)
225	0.48(0.05)	0.00(0.00)	0.00(0.00)	0.00(0.00)	0.00(0.00)	0.47(0.05)
250	0.47(0.04)	0.00(0.00)	0.00(0.00)	0.00(0.00)	0.00(0.00)	0.47(0.04)

Table 4: Table corresponding to Figure 25, Mean and standard deviation (among parentheses) of each of the subplot in the figure.

Figure 25 is drawn with the same procedure, but the item 3. is substituted by

3' for all the (β_1, t) square where the hypothesis of Bm cannot be rejected.

In Figure 24 the Gaussian hypothesis holds nearly always on the higher length time windows. This is expected, because the wider the window, the more stable the long-term parameter H. Remarkably, it always holds in the intra-break zone III. On the opposite, it does not hold on all but the last length on the entire time series. It can be concluded that the increase of the time length allows the convergence to the gaussian. It is also worth remarking that on the entire time series the effect of non-Gaussianity of some intra-break zone (in I-V) at the lowest time lengths is stronger than the Gaussians ones, so the entire time series ("all") is not Gaussian either. Similar remarks hold for the Bm hypothesis 25. Moreover, on some intra-break zones the appearance of Bm is too low for showing an histogram.

For what concerns the forecast, Table 5 sums up the percentages of success of Bm versus the fBm forecast.

Figures 26-35 show the results for each fixed length of the time series, corresponding to the Figures 12-21. Refer also to Table 5, where results are resumed. The percentage of

	I		II		III		IV		V		all	
	Bm	fBm	Bm	fBm	Bm	fBm	Bm	fBm	Bm	fBm	Bm	fBm
25	0.264	0.122	0.286	0.130	0.269	0.149	0.211	0.108	0.258	0.065	0.260	0.115
50	0.315	0.128	0.368	0.131	0.341	0.131	0.261	0.097	0.284	0.063	0.316	0.113
75	0.328	0.139	0.388	0.128	0.356	0.137	0.278	0.086	0.292	0.059	0.331	0.114
100	0.330	0.143	0.392	0.127	0.374	0.123	0.280	0.085	0.294	0.058	0.335	0.114
125	0.332	0.143	0.389	0.132	0.370	0.129	0.280	0.085	0.294	0.058	0.334	0.116
150	0.327	0.148	0.388	0.133	0.374	0.125	0.280	0.085	0.294	0.058	0.332	0.117
175	0.334	0.141	0.389	0.133	0.372	0.127	0.280	0.085	0.294	0.058	0.335	0.115
200	0.337	0.139	0.388	0.133	0.368	0.131	0.280	0.085	0.294	0.058	0.335	0.115
225	0.339	0.139	0.388	0.133	0.372	0.127	0.280	0.085	0.294	0.058	0.337	0.114
250	0.343	0.138	0.388	0.133	0.372	0.127	0.280	0.085	0.294	0.058	0.338	0.114

Table 5: The table sums up the results corresponding to the Figures 26-35. The rows show the results depending on the time length. The columns report the intra-break time zones. Each column is divided into two parts: the two numbers represent the percentages of best performance of the Bm, and of the fBm, compared on the total amount of time windows selected in the (β_1, t) space for performing the forecast.

windows where the forecast was not performed is not shown in Table 5, because it is the complement to 1 of the sum of the $fBm + Bm$ numbers. The forecast performed through Bm performs clearly better than the one based on fBm. This result allows to state that the first 5 days after a Bm window are well suitable for being still modeled through a Bm.

It can be seen that inside each intra-break zone, the percentage of prevailence of Bm versus Bm does not dramatically depend on the time length, since it remains nearly constant across all the time lengths. Instead, there is quite a difference among the intra-break zones I-IV and V: in the first zones the proportion Bm versus fBm is approximately a bit more than 2:1, so the Bm forecast is better than the fBm one twice of the times. In zone V the proportion jumps to more than 3:1, so pointing out an increase of the validity of the Bm. Of course, the percentages corresponding to the entire time series is a mean of the ones calculated on the intra-break zones and shows a proportion of approximately 2:1 for the smallest length, and 3:1 for the rest.

6 Conclusions

This paper deals with the analysis of the long-run properties of portfolios of commodities through the estimation of the long-term parameter H. The empirical data refer to Brent and Dubai oil, with the addition of WTI as reference commodity.

A wide set of rolling time windows over a ten years dataset have been explored, with different lengths. Some specific portfolios have been taken into account, and the remarkable cases of Brownian motion and stationarity have been discussed. Results state that the long-term memory properties of the mispricing portfolios stabilize when the time period of the analysis enlarges. Furthermore, forecasting rules in long- and short-term have been deeply discussed.

The selection of eleven reference portfolios allows to overcross the computational complexity of the problem. However, operational research procedures able to reduce the cardinality of the investigation set without losing much information should be implemented

in order to obtain a paramount view of the long-term memory property of the considered commodities portfolios.

References

Alvarez-Ramirez, J., Alvarez, J., and Rodriguez, E. (2008). Short-term predictability of crude oil markets: a detrended fluctuation analysis approach. *Energy Economics*, 30(5):2645–2656.

Alvarez-Ramirez, J., Cisneros, M., Ibarra-Valdez, C., and Soriano, A. (2002). Multifractal Hurst analysis of crude oil prices. *Physica A*, 313(3):651–670.

Ausloos, M. (2002). Financial time series and statistical mechanics. In *Computational Statistical Physics*, pages 153–168. Springer.

Baillie, R. T. (1996). Long memory processes and fractional integration in econometrics. *Journal of Econometrics*, 73(1):5–59.

Bardet, J.-M., Lang, G., Oppenheim, G., Philippe, A., Stoev, S., and Taqqu, M. S. (2003). Semi-parametric estimation of the long-range dependence parameter: a survey. *Theory and applications of long-range dependence*, pages 557–577.

Barsky, R. B. and Kilian, L. (2004). Oil and the macroeconomy since the 1970s. *The Journal of Economic Perspectives*, 18(4):115–134.

Cajueiro, D. O. and Tabak, B. M. (2004). The Hurst exponent over time: testing the assertion that emerging markets are becoming more efficient. *Physica A*, 336(3):521–537.

Corazza, M. and Malliaris, A. T. G. (2002). Multi-fractality in foreign currency markets. *Multinational Finance Journal*, 6(2):65–98.

Ferraro, D., Rogoff, K., and Rossi, B. (2015). Can oil prices forecast exchange rates? an empirical analysis of the relationship between commodity prices and exchange rates. *Journal of International Money and Finance*, 54:116–141.

Gregory, A. and Hansen, B. (1996). Residual-based tests for cointegration in models with regime shift. *Journal of Economics*, 70:99–126.

Hurst, H. E. (1951). Long-term storage capacity of reservoirs. *Transactions of the American Society of Civil Engineers*, 116:770–808.

Istas, J. and Lang, G. (1997). Quadratic variations and estimation of the local hölder index of a gaussian process. In *Annales de l'Institut Henri Poincare (B) Probability and Statistics*, volume 33, pages 407–436. Elsevier.

J.P., S. and Sella, P. (2008). On the distribution of returns and memory effects in indian capital markets. *International Research Journal of Finance and Economics*, I(14):165–176.

Kilian, L. (2009). Not all oil price shocks are alike: Disentangling demand and supply shocks in the crude oil market. *The American economic review*, 99(3):1053–1069.

Kirichenko, L., Radivilova, T., and Deineko, Z. (2011). Comparative analysis for estimating of the Hurst exponent for stationary and nonstationary time series. *Information Technologies & Knowledge*, 5(1):371–388.

Kristoufek, L. and Vosvrda, M. (2014). Commodity futures and market efficiency. *Energy Economics*, 42:50–57.

Kyaw, N. A., Los, C. A., and Zong, S. (2006). Persistence characteristics of Latin American financial markets. *Journal of Multinational Financial Management*, 16(3):269–290.

Little, M., McSharry, P., Moroz, I., and Roberts, S. (2006). Nonlinear, biophysically-informed speech pathology detection. In *Acoustics, Speech and Signal Processing, 2006. ICASSP 2006 Proceedings. 2006 IEEE International Conference on. Free download of the subroutine from http://www.maxlittle.net/software*, volume 2, pages II–II. IEEE.

online manual, M. (2006). Matlab reference manual. $https : //it.mathworks.com/help/wavelet/ref/wfbmesti.html?searchHighlight = wfbmesti\&s_tid = doc_srchtitle$.

Ortiz-Cruz, A., Rodriguez, E., Ibarra-Valdez, C., and Alvarez-Ramirez, J. (2012). Efficiency of crude oil markets: Evidences from informational entropy analysis. *Energy Policy*, 41:365–373.

Potgieter, P. H. (2009). Fractal asset returns, arbitrage and option pricing. *Chaos, Solitons & Fractals*, 42(3):1792–1795.

Serletis, A. and Andreadis, I. (2004). Random fractal structures in North American energy markets. *Energy Economics*, 26(3):389–399.

Stock, J. H. and Watson, M. W. (2003). *Introduction to econometrics*, volume 104. Addison Wesley Boston.

Tabak, B. M. and Cajueiro, D. O. (2007). Are the crude oil markets becoming weakly efficient over time? A test for time-varying long-range dependence in prices and volatility. *Energy Economics*, 29(1):28–36.

Vidyamurthy, G. (2004). *Pairs Trading: quantitative methods and analysis*. John Wiley & Sons.

Wang, Y. and Liu, L. (2010). Is WTI crude oil market becoming weakly efficient over time?: New evidence from multiscale analysis based on detrended fluctuation analysis. *Energy Economics*, 32(5):987–992.

7   Appendix: Comparison among subroutines for the estimate of H

An issue that had to be faced has been the selection of a method for the estimate of H. While a comparative study on the best performing method for the estimate of H on short time series is out of the scope of this paper, still the availability of a reliable estimate method is very relevant for the development of the numerical analyses presented. Actually, there

length	w1	w2	w3	$fastdfa$
25	0.0088 (0.31)	0.2543 (0.57)	0.5699 (0.34)	0.0741 (0.17)
50	0.0027 (0.22)	0.0238 (0.23)	0.8360 (0.23)	0.0832 (0.11)
75	0.0006 (0.18)	0.0039 (0.17)	1.5449 (0.28)	0.0480 (0.11)
100	0.0008 (0.16)	0.0041 (0.14)	0.9370 (0.18)	0.0554 (0.08)
125	0.0015 (0.14)	0.0029 (0.13)	0.9605 (0.16)	0.0272 (0.08)
150	0.0014 (0.13)	0.0028 (0.11)	1.3371 (0.25)	0.0004 (0.08)
175	0.0020 (0.12)	0.0022 (0.10)	1.0749 (0.17)	0.0071 (0.07)
200	0.0030 (0.11)	0.0030 (0.09)	1.2479 (0.17)	0.0374 (0.06)
225	0.0041 (0.11)	0.0042 (0.09)	0.9549 (0.13)	0.0300 (0.07)
250	0.0034 (0.10)	0.0034 (0.08)	0.9844 (0.13)	0.0034 (0.06)

Table 6: Analysis of the precision of the subroutines estimating H in the uncorrelated case. The first column reports the time series length. The others report the absolute value of the distance from the theoretical value and the standard deviation of the outputs of: I, II and III output of wfbmesti (columns w1, w2, and w3), and fastdfa

is an entire branch of literature dealing with the properties of the numerical estimators of H and related algorithms. From literature, we already know that the DFA and wavelet methods perform better than the R/S analysis on time series longer than 500 (Kirichenko et al. (2011)). Therefore, the main issue was to refine the results of the litarature on the precision of the estimate of implemented algorithms when the time series are short.
First, we define a set of lengths Δ_l, with $l = 1, \ldots, 10$ and
$(\Delta_1, \ldots, \Delta_{10}) = (25, 50, 75, 100, 125, 150, 175, 200, 225, 250)$, that basically catch the trading month (25 days) and its multiples, and it is fine enough to guarantee a detailed analysis. For each length in Δ_l, we have performed a numerical estimate of the mean and of the standard deviation of H for the focus cases $H = 0$ (uncorrelated data) and $H = 0.5$ (Bm). Second, we focuse on the algorithms that are implemented in the MATLAB subroutines $fastdfa$ (Little et al. (2006)) and $wfbmesti$ (online manual (2006)), which actually provides three different estimates. The first two (w1 and w2) are based on second order discrete derivative, the second one is the wavelet-based. The third estimate (w3) is based on the linear regression in loglog plot, of the variance of detail versus level. Therefore, we extended the analysis to the four subroutines. Table 1reports a comparison among w1, w2, w3 and $fastdfa$ in the uncorrelated case, for various lengths of the time series. Each value has been calculated on 10000 simulations of uncorrelated random variables. The columns report the mean of the absolute value of the distance from the theoretical value, and, among parentheses, the standard deviation of the estimated H from the theoretical H. It is immediately visible that the mean most close to the theoretical one is given by w1, while the lowest standard deviation is given by $fastdfa$. w3 gives the highest error, and the standard deviations are higher than w1. w2 has a standard deviation lower than w1, but bigger than $fastdfa$. Moreover, the mean errors of w2 are higher than w1, so the best choices are either w1 (lower error) or $fastdfa$ (lower standard deviation).
Table 2 reports the analogous comparison for the Brownian motion case. Once more, w1 gives the lowest error. Moreover, also the standard deviaton is lower. Since we need to adopt a single method for comparing all the numerical analysis, we selected w1 as estimator in our simulations.

The algorithm used for calculating w1 is described in Istas and Lang Istas and Lang

length	w1	w2	w3	fastdfa
25	0.0113 (0.28)	0.1394 (0.58)	0.1152 (0.34)	0.1377 (0.28)
50	0.0049 (0.19)	0.0193 (0.25)	0.1441 (0.23)	0.0663 (0.20)
75	0.0024 (0.16)	0.0070 (0.19)	0.3275 (0.28)	0.1695 (0.21)
100	0.0026 (0.14)	0.0059 (0.16)	0.1332 (0.18)	0.0585 (0.15)
125	0.0026 (0.12)	0.0043 (0.14)	0.0425 (0.16)	0.1334 (0.16)
150	0.0024 (0.11)	0.0041 (0.12)	0.2276 (0.25)	0.0836 (0.15)
175	0.0020 (0.11)	0.0032 (0.11)	0.1105 (0.17)	0.1127 (0.13)
200	0.0025 (0.10)	0.0029 (0.11)	0.1716 (0.17)	0.0521 (0.12)
225	0.0027 (0.09)	0.0034 (0.10)	0.0942 (0.13)	0.1172 (0.13)
250	0.0023 (0.09)	0.0028 (0.09)	0.0564 (0.13)	0.0724 (0.13)

Table 7: Analysis of the precision of the subroutines estimating H in the Bm case. The first column reports the time series length. The others report the absolute value of the distance from the theoretical value and the standard deviation of the outputs of: I, II and III output of wfbmesti (columns w1, w2, and w3), and fastdfa

(1997), where H is estimated as the local H *older* index $\hat{h}$ of a Gaussian process, using a discrete observation of one sample path.

We define $y(t) = M_{t+1} - M_t$, for each t, and build the empirical quadratic variation $U(a, n, \Delta) = \frac{1}{n} \sum_{j=1}^{n-p} (\sum_{i=0}^{p} a_i y((i+j)\Delta))^2$. Istas and Lang prove that selecting two sequences $a^{(1)}$ and $a^{(2)}$ with *double time mesh*, i.e. the sequence defined by $a_{2i}^{(2)} = a_i^{(1)}$ and $a_{2i+1}^{(2)} = 0$ for $0 \leq i \leq p$, and under mild assumptions for $a^{(1)}$ (Assumption A2 at p.412 in Istas and Lang (1997)), one obtains an estimator $\hat{h}$ of H given by

$$\hat{h} = \frac{1}{2} log_2 \left(\frac{U(a^{(2)}, n, \Delta)}{U(a^{(1)}, n, \Delta)} \right). \tag{6}$$

The parameters used are $\Delta = 1$ and $a^{(1)} = (1, -2, 1)$, that correspond to the second order discrete derivative of $y(t)$. This specific choice is just one of the many satisfying the Assumption (A2 in Istas and Lang (1997)). The same paper reports an analysis of the mean square error (MSE) of the estimate depending on the length of the time series under examination. Unfortunately, the authors start from a minimal length of 512, that corresponds on daily data to nearly two years: definitively, too long for capturing phenomena that may last one month, only. The bounds $m \pm \sigma$ are used in the next data analysis to fix the confidence intervals, where m is the estimate of H through w1, and σ are the values among parentheses in the corresponding columns of Tables 1 and 2. The hypothesis of uncorrelated data is not rejected if $H \in (-\sigma, +\sigma)$; the hypothesis of Bm is not rejected if $H \in (0.5 - \sigma, 0.5 + \sigma)$.
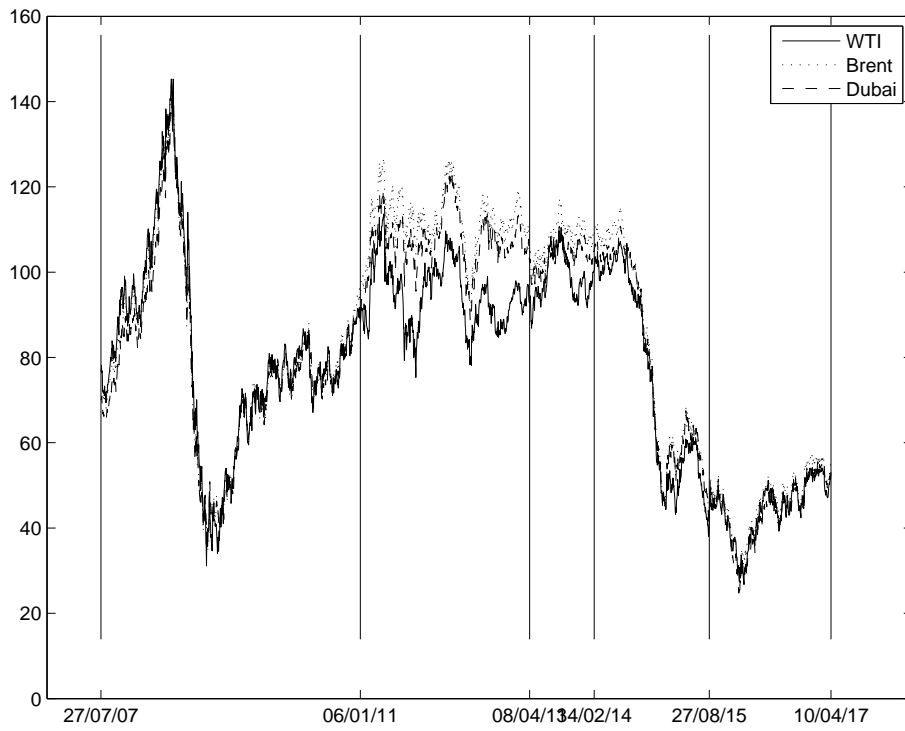
Figure 1: Plot of the time series WTI, Brent, Dubai, and the corresponding structural breaks.
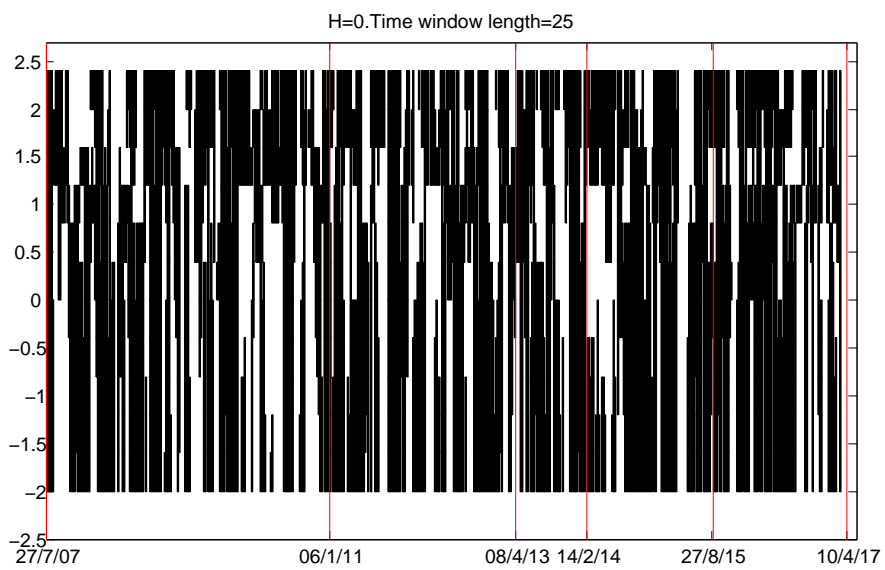
Figure 2: Time-parameter plane. The black rectangles which left−bottom corner is given by (t, β_1) evidence the combination of parameter and time where the hypothesis of uncorrelation of the mispricing calculated parameter β_1 cannot be rejected on time windows of length 25, starting at time t. The vertical lines point out the structural breaks.
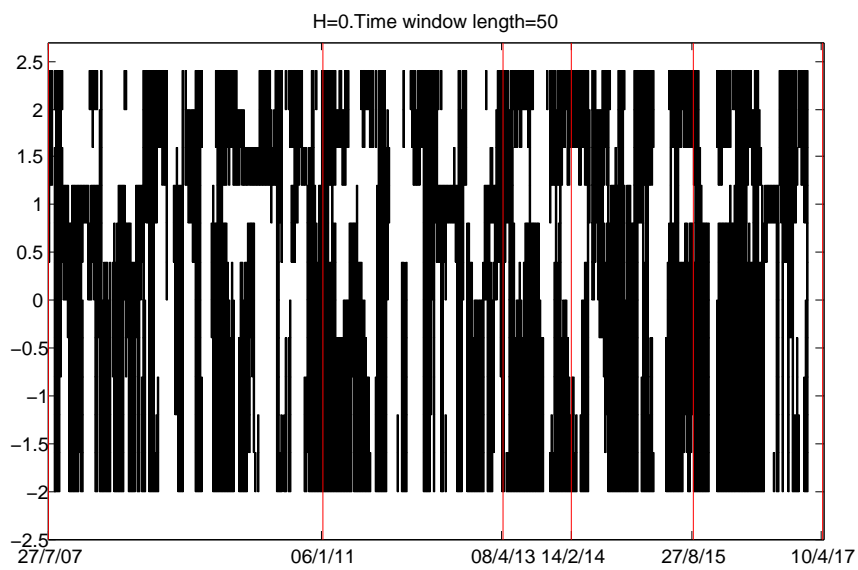
Figure 3: Time-parameter plane. The black rectangles which left−bottom corner is given by (t, β_1) evidence the combination of parameter and time where the hypothesis of uncorrelation of the mispricing calculated parameter β_1 cannot be rejected on time windows of length 50, starting at time t. The vertical lines point out the structural breaks.
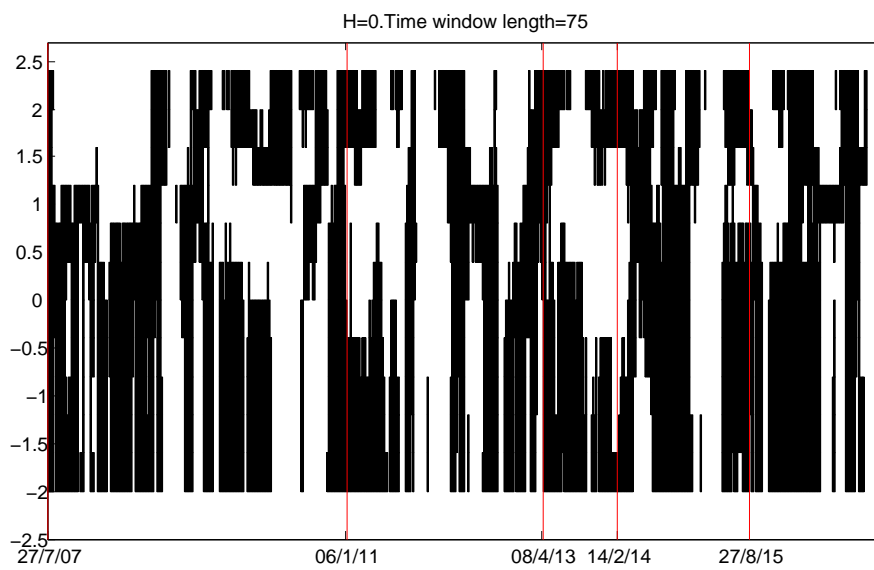
Figure 4: Time-parameter plane. The black rectangles which left−bottom corner is given by (t, β_1) evidence the combination of parameter and time where the hypothesis of uncorrelation of the mispricing calculated parameter β_1 cannot be rejected on time windows of length 75, starting at time t. The vertical lines point out the structural breaks.
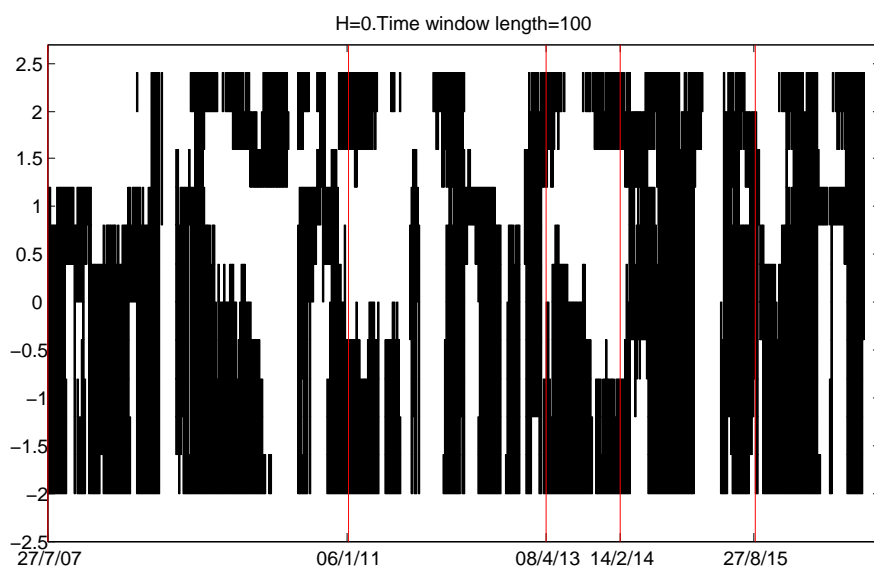
Figure 5: Time-parameter plane. The black rectangles which left−bottom corner is given by (t, β_1) evidence the combination of parameter and time where the hypothesis of uncorrelation of the mispricing calculated parameter β_1 cannot be rejected on time windows of length 100, starting at time t. The vertical lines point out the structural breaks.
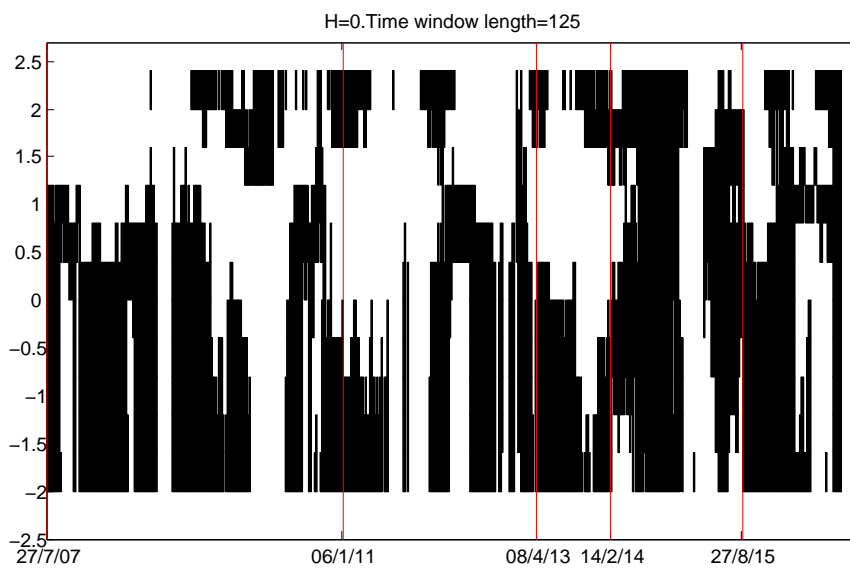
Figure 6: Time-parameter plane. The black rectangles which left−bottom corner is given by (t, β_1) evidence the combination of parameter and time where the hypothesis of uncorrelation of the mispricing calculated parameter β_1 cannot be rejected on time windows of length 125, starting at time t. The vertical lines point out the structural breaks.
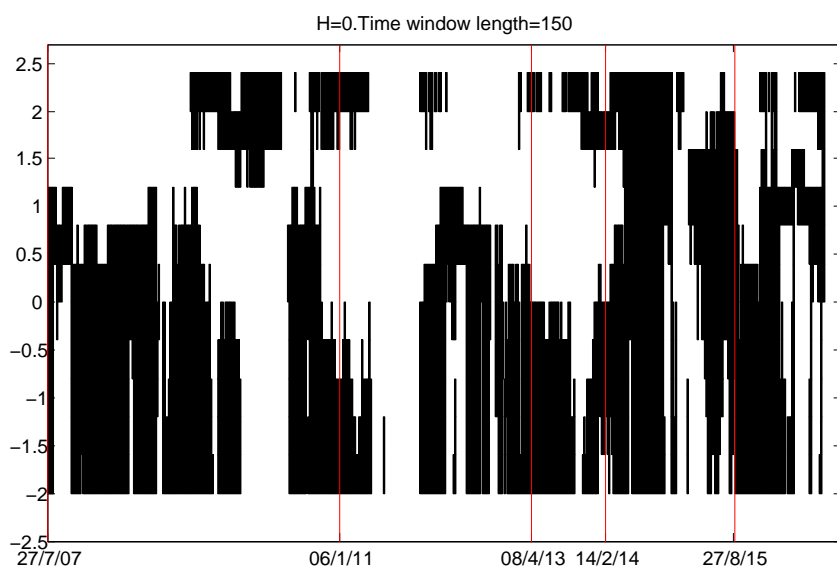
Figure 7: Time-parameter plane. The black rectangles which left−bottom corner is given by (t, β_1) evidence the combination of parameter and time where the hypothesis of uncorrelation of the mispricing calculated parameter β_1 cannot be rejected on time windows of length 150, starting at time t. The vertical lines point out the structural breaks.

26
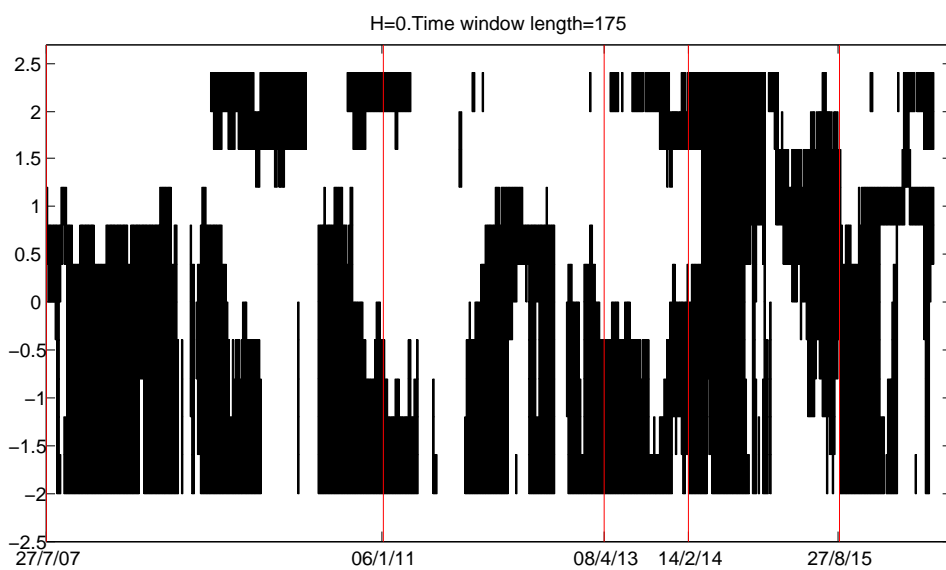
Figure 8: Time-parameter plane. The black rectangles which left−bottom corner is given by (t, β_1) evidence the combination of parameter and time where the hypothesis of uncorrelation of the mispricing calculated parameter β_1 cannot be rejected on time windows of length 175, starting at time t. The vertical lines point out the structural breaks.
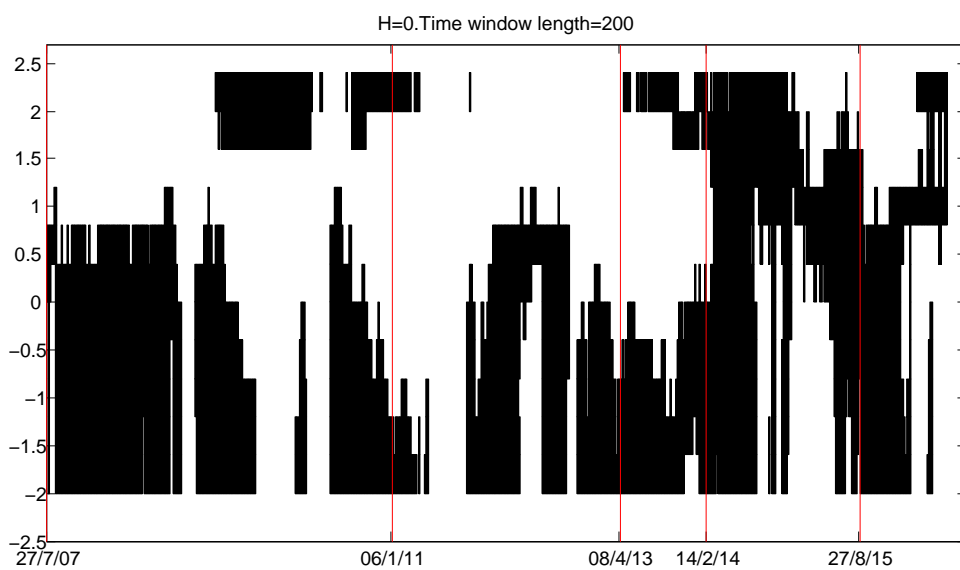
Figure 9: Time-parameter plane. The black rectangles which left−bottom corner is given by (t, β_1) evidence the combination of parameter and time where the hypothesis of uncorrelation of the mispricing calculated parameter β_1 cannot be rejected on time windows of length 200, starting at time t. The vertical lines point out the structural breaks.

28
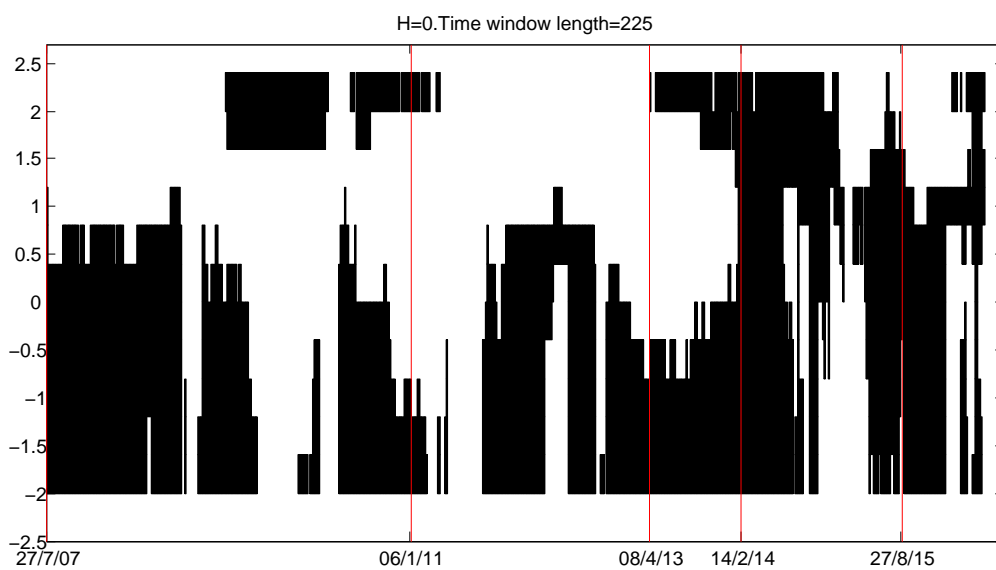
Figure 10: Time-parameter plane. The black rectangles which left−bottom corner is given by (t, β_1) evidence the combination of parameter and time where the hypothesis of uncorrelation of the mispricing calculated parameter β_1 cannot be rejected on time windows of length 225, starting at time t. The vertical lines point out the structural breaks.
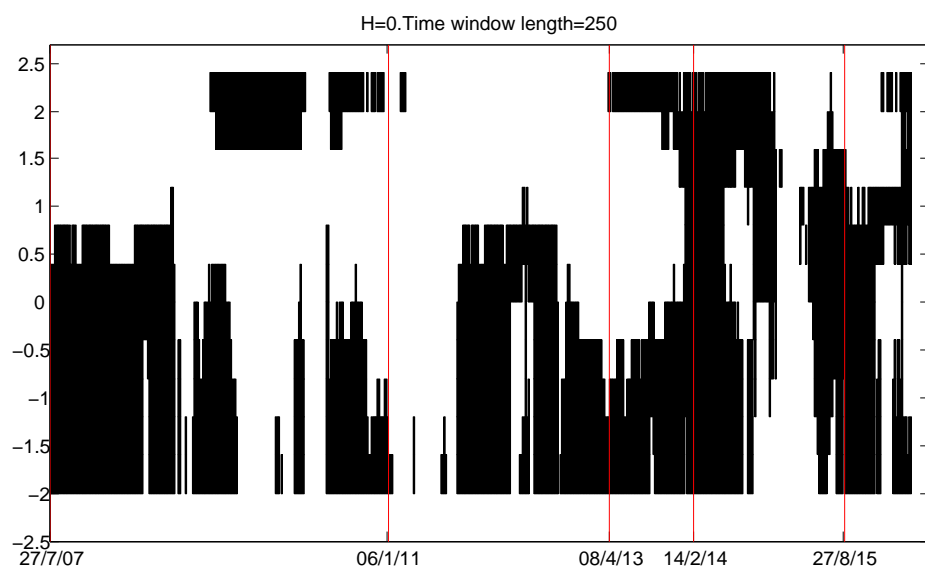
Figure 11: Time-parameter plane. The black rectangles which left−bottom corner is given by (t, β_1) evidence the combination of parameter and time where the hypothesis of uncor-relation of the mispricing calculated parameter β_1 cannot be rejected on time windows of length 250, starting at time t. The vertical lines point out the structural breaks.

30
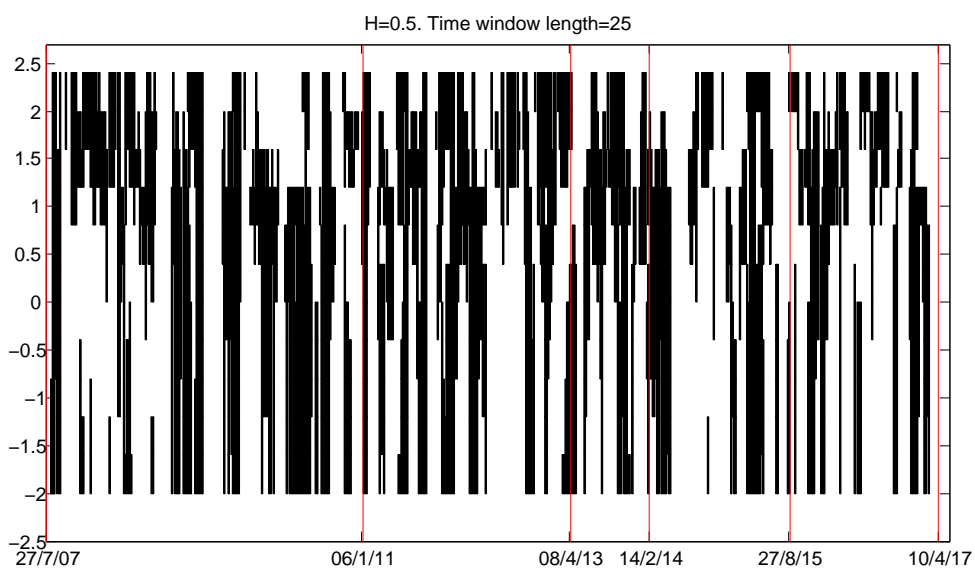
Figure 12: Time-parameter plane. The black rectangles which left−bottom corner is given by (t, β_1) evidence the combination of parameter and time where the hypothesis of Bm of the mispricing calculated parameter β_1 cannot be rejected on time windows of length 25, starting at time t. The vertical lines point out the structural breaks.
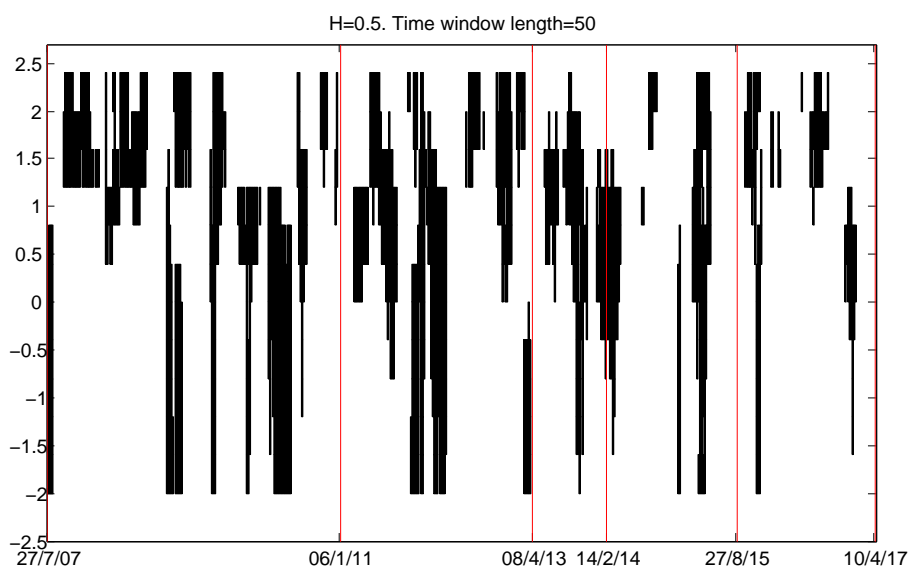
Figure 13: Time-parameter plane. The black rectangles which left−bottom corner is given by (t, β_1) evidence the combination of parameter and time where the hypothesis of Bm of the mispricing calculated parameter β_1 cannot be rejected on time windows of length 50, starting at time t. The vertical lines point out the structural breaks.

32
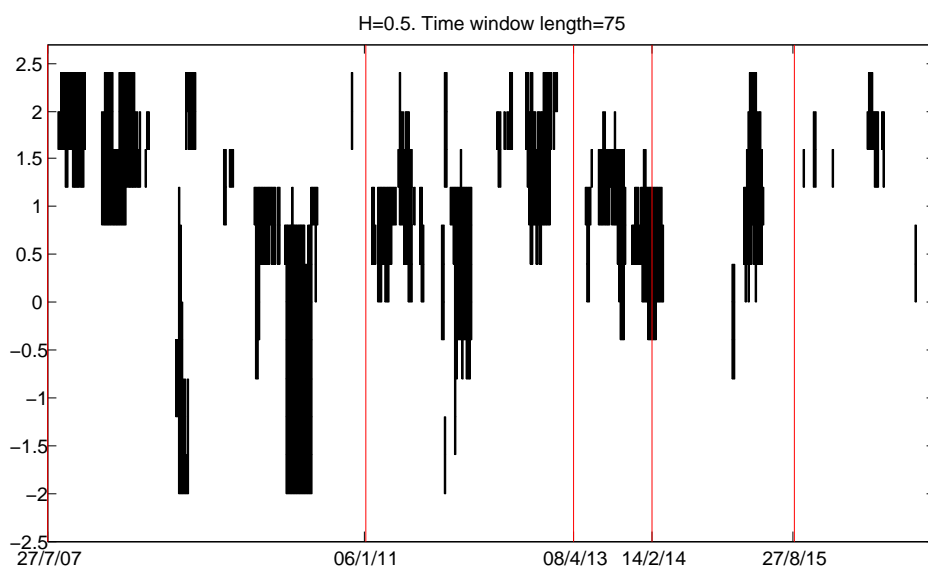
Figure 14: Time-parameter plane. The black rectangles which left−bottom corner is given by (t, β_1) evidence the combination of parameter and time where the hypothesis of Bm of the mispricing calculated parameter β_1 cannot be rejected on time windows of length 75, starting at time t. The vertical lines point out the structural breaks.
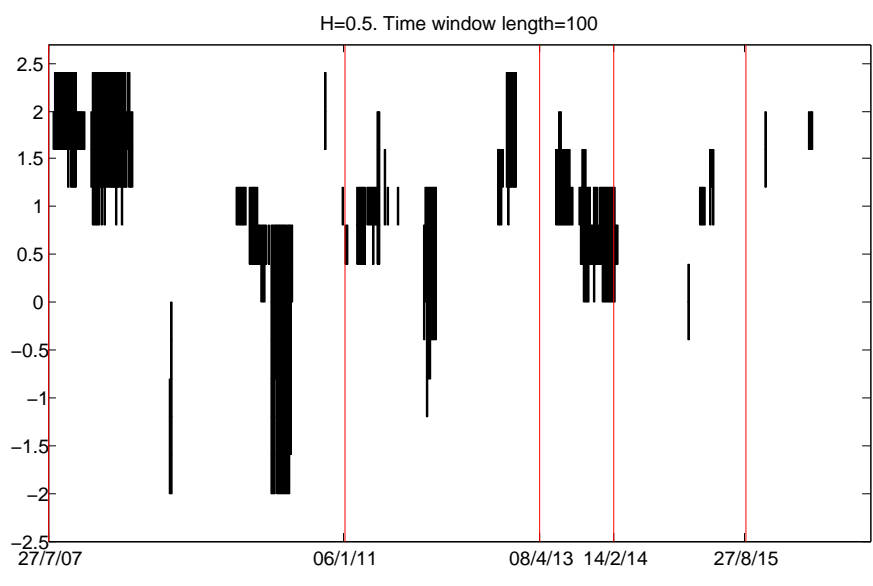
Figure 15: Time-parameter plane. The black rectangles which left−bottom corner is given by (t, β_1) evidence the combination of parameter and time where the hypothesis of Bm of the mispricing calculated parameter β_1 cannot be rejected on time windows of length 25, starting at time t. The vertical lines point out the structural breaks.
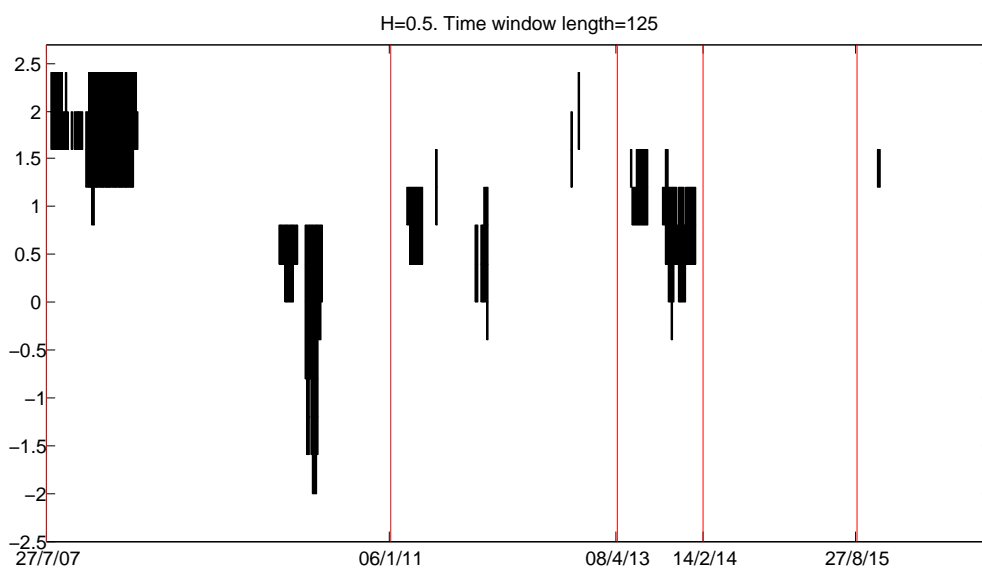
Figure 16: Time-parameter plane. The black rectangles which left−bottom corner is given by (t, β_1) evidence the combination of parameter and time where the hypothesis of Bm of the mispricing calculated parameter β_1 cannot be rejected on time windows of length 125, starting at time t. The vertical lines point out the structural breaks.
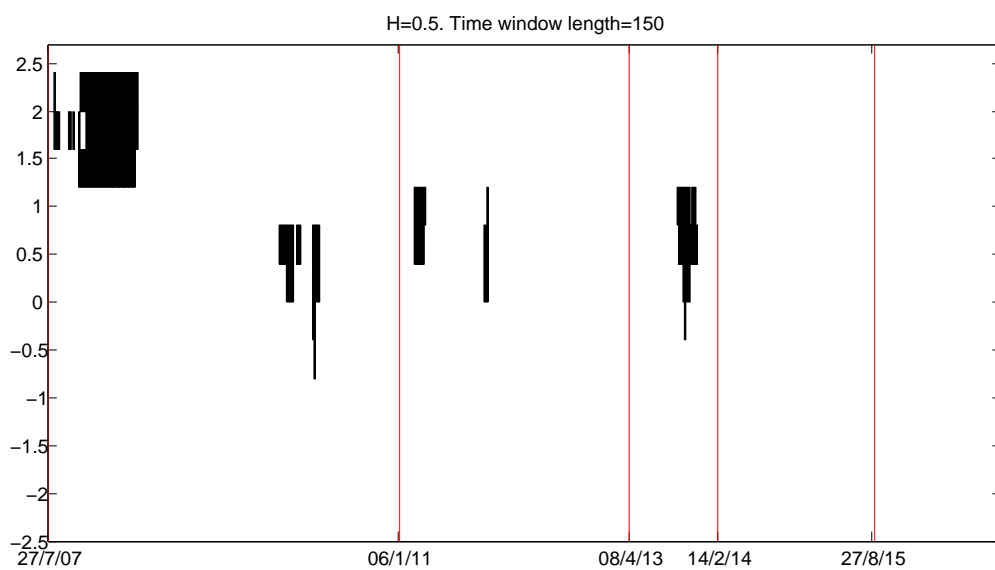
Figure 17: Time-parameter plane. The black rectangles which left−bottom corner is given by (t, β_1) evidence the combination of parameter and time where the hypothesis of Bm of the mispricing calculated parameter β_1 cannot be rejected on time windows of length 150, starting at time t. The vertical lines point out the structural breaks.
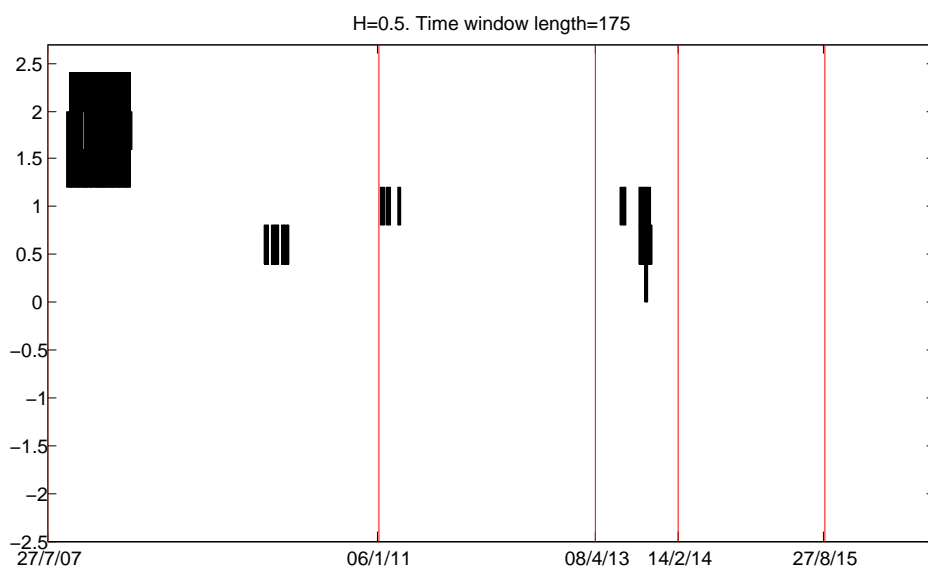
Figure 18: Time-parameter plane. The black rectangles which left−bottom corner is given by (t, β_1) evidence the combination of parameter and time where the hypothesis of Bm of the mispricing calculated parameter β_1 cannot be rejected on time windows of length 175, starting at time t. The vertical lines point out the structural breaks.
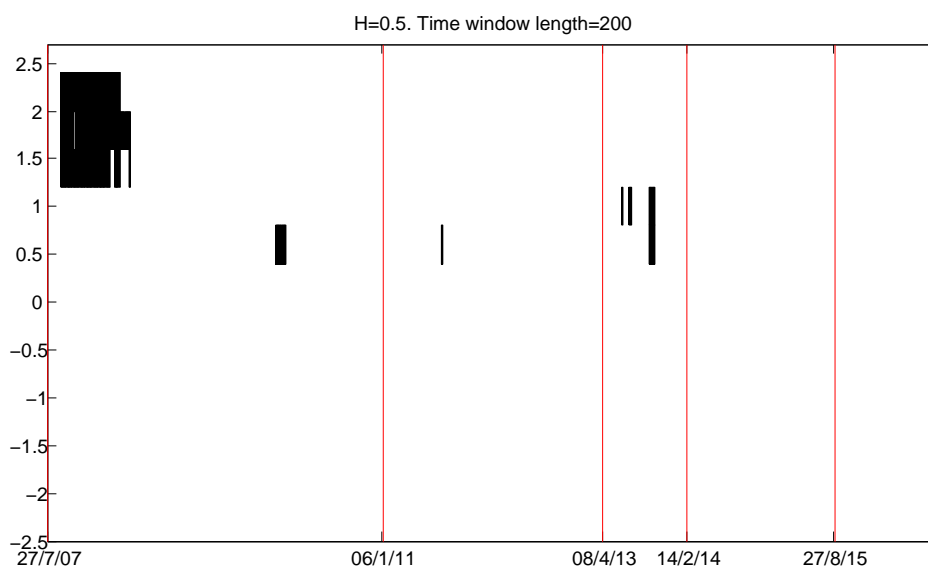
Figure 19: Time-parameter plane. The black rectangles which left−bottom corner is given by (t, β_1) evidence the combination of parameter and time where the hypothesis of Bm of the mispricing calculated parameter β_1 cannot be rejected on time windows of length 200, starting at time t. The vertical lines point out the structural breaks.
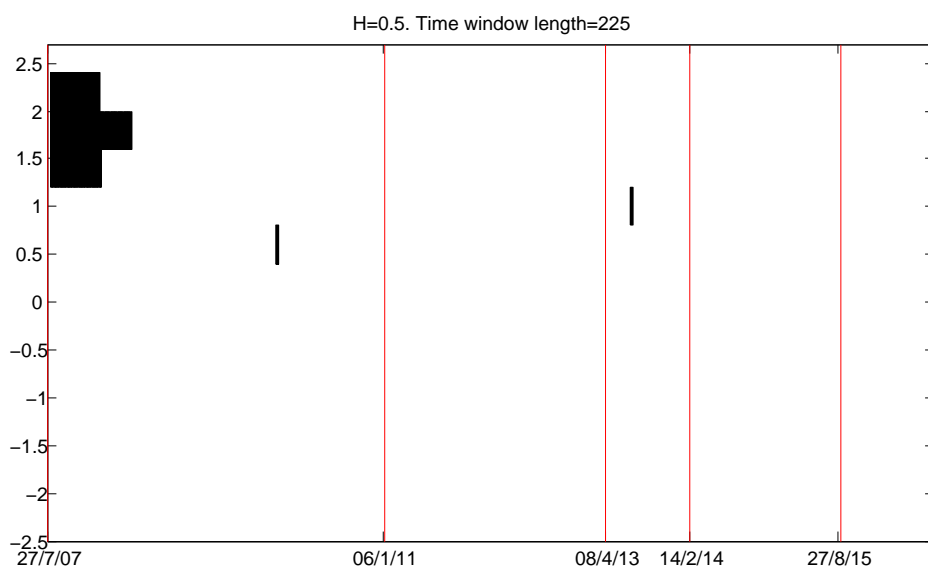
Figure 20: Time-parameter plane. The black rectangles which left−bottom corner is given by (t, β_1) evidence the combination of parameter and time where the hypothesis of Bm of the mispricing calculated parameter β_1 cannot be rejected on time windows of length 225, starting at time t. The vertical lines point out the structural breaks.
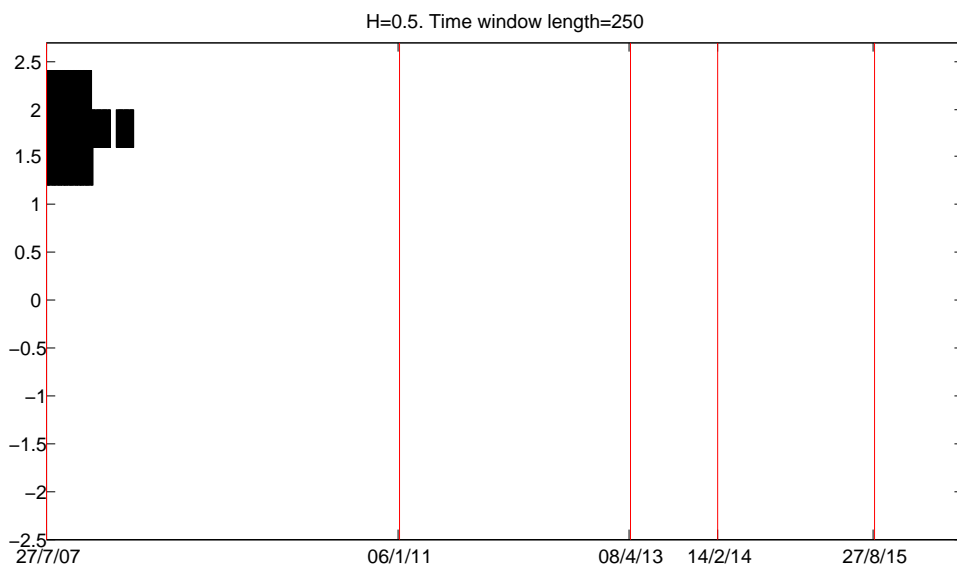
Figure 21: Time-parameter plane. The black rectangles which left−bottom corner is given by (t, β_1) evidence the combination of parameter and time where the hypothesis of Bm of the mispricing calculated parameter β_1 cannot be rejected on time windows of length 250, starting at time t. The vertical lines point out the structural breaks.
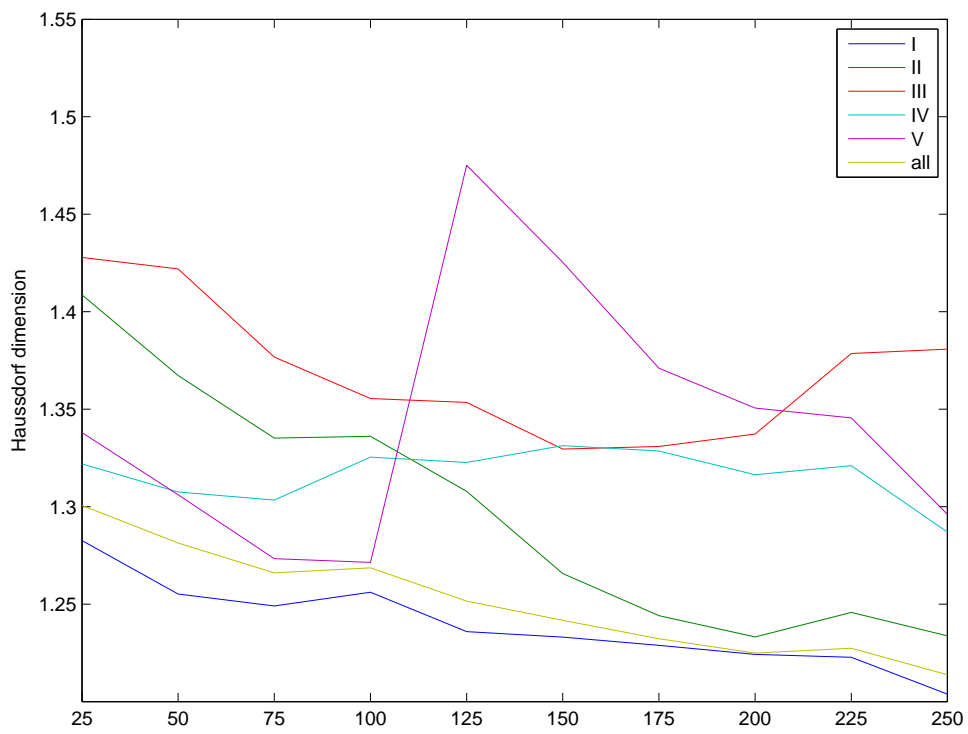
Figure 22: Evolution of the Haussdorf dimension on the subseries as the length of the time window increases. This figure corresponds to the values in 5.
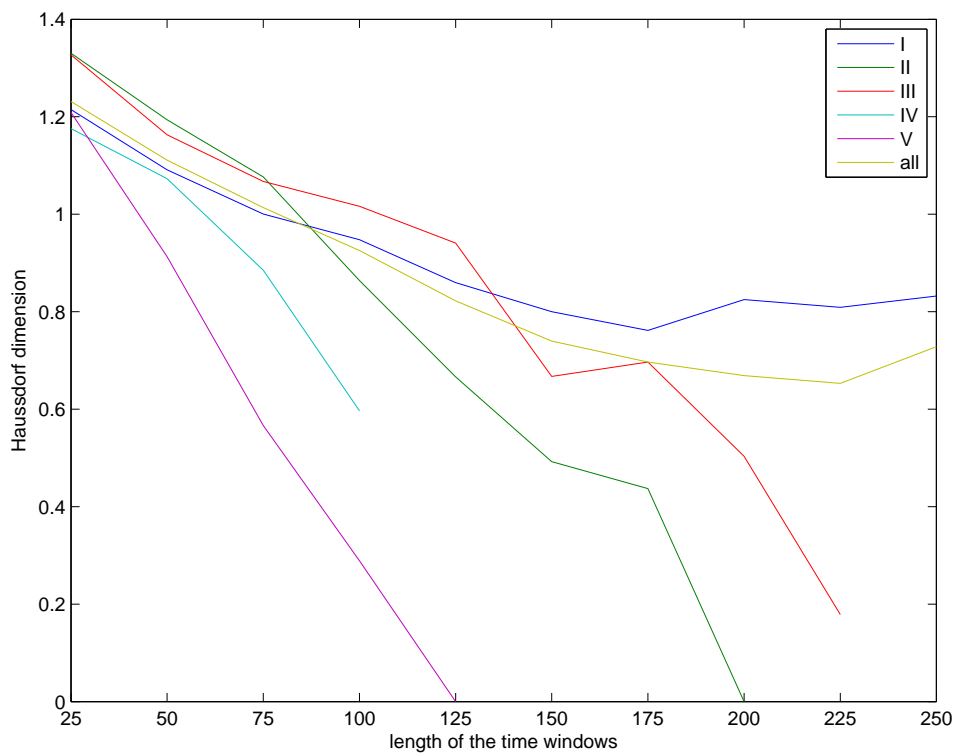
Figure 23: Evolution of the Haussdorf dimension on the subseries as the length of the time window increases. This figure corresponds to the values in 5. The time series that stop before the end cannot be calculated due to a too low occupancy of the figure, and actually result in 0 dimension (no black zones).
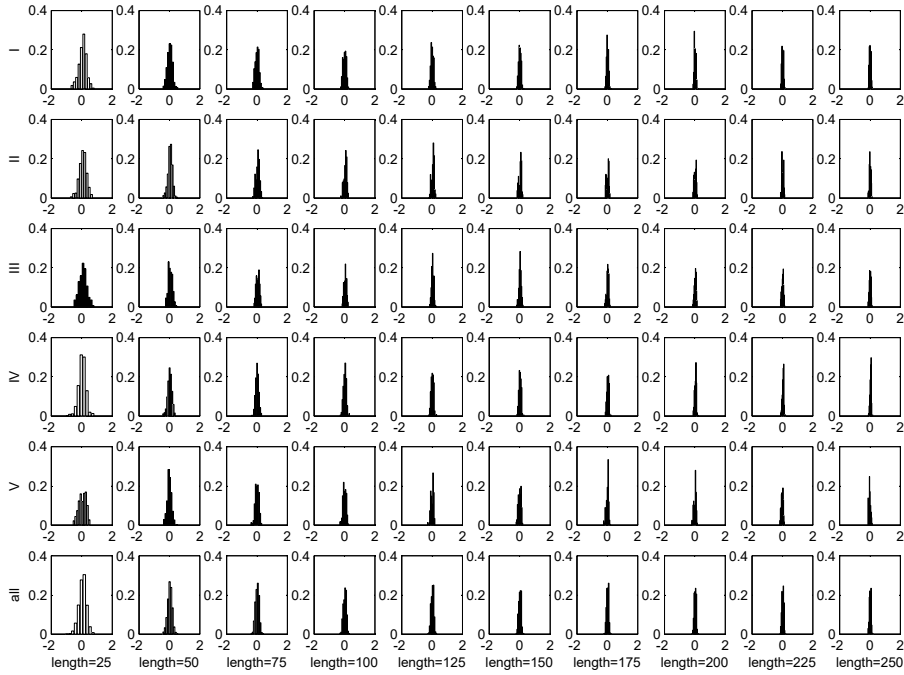
Figure 24: Conditional probability to measure H equal to the value reported in the x-axis, knowing that in the previous window H was in the confidence interval of 0. The Jarque-Bera test of normality was done on such empirical distribution. The figures in black don't reject the Gaussian hypothesis, the figures in white do reject it. The rows report the measurement for the corresponding intra-structural break time window. The columns divide the measurement depending on the length of the time series where H has been estimated.
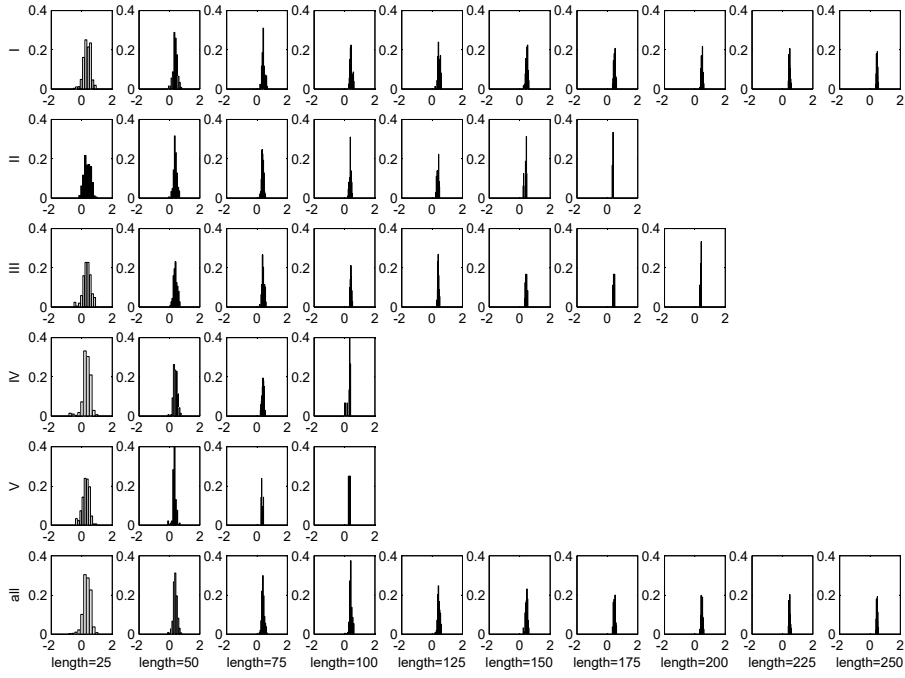
Figure 25: Conditional probability to measure H equal to the value reported in the x-axis, knowing that in the previous window H was in the confidence interval of 0.5. The Jarque-Bera test of normality was done on such empirical distribution. The figures in black don't reject the Gaussian hypothesis, the figures in white do reject it. The rows report the measurement for the corresponding intra-structural break time window. The columns divide the measurement depending on the length of the time series where H has been estimated.
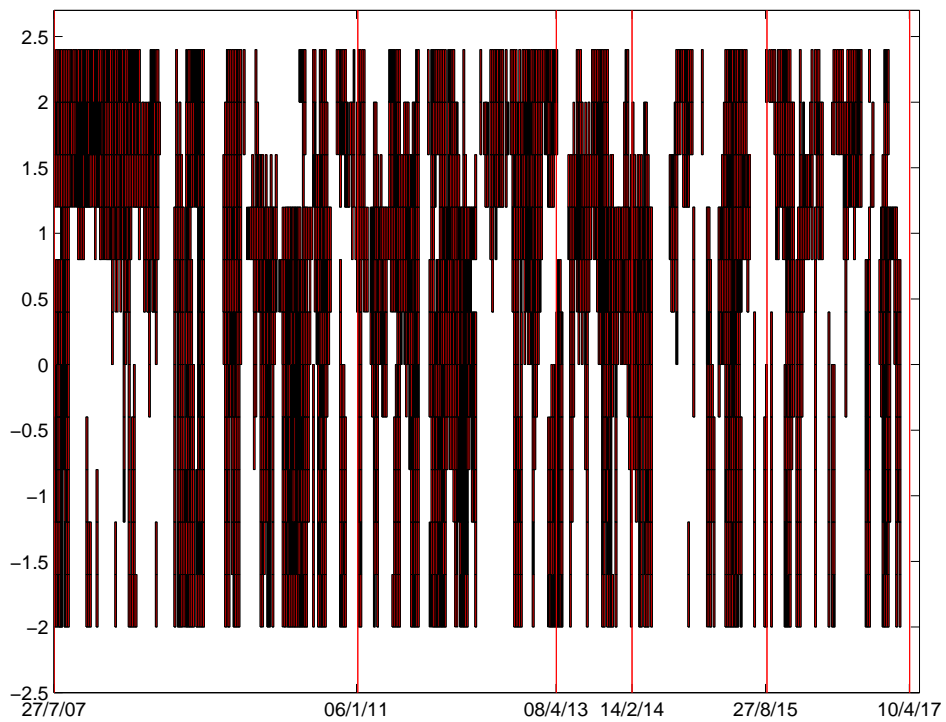
Figure 26: Forecast on the 5 days following a Bm time windows of length 25. The red squares at position (β_1, t) evidence that the forecast of the 5 days following a Bm time window of length 25, starting at time t and characterized by the same parameter β_1 is better than the fBm one with H proper of the window starting at $t+5$, with the same β_1, and same length. Table 5 sums up the percentages of prevalence
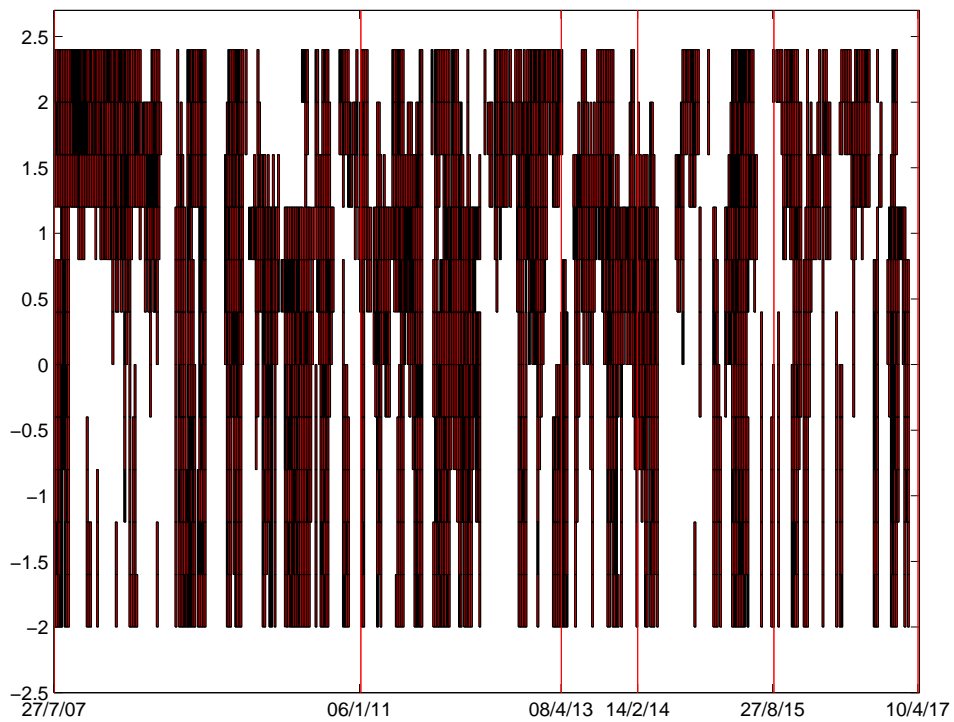
Figure 27: Forecast on the 5 days following a Bm time windows of length 50. The red squares at position (β_1, t) evidence that the forecast of the 5 days following a Bm time window of length 50, starting at time t and characterized by the same parameter β_1) is better than the fBm one with H proper of the window starting at $t+5$, with the same β_1, and same length. Table 5 sums up the percentages of prevalence
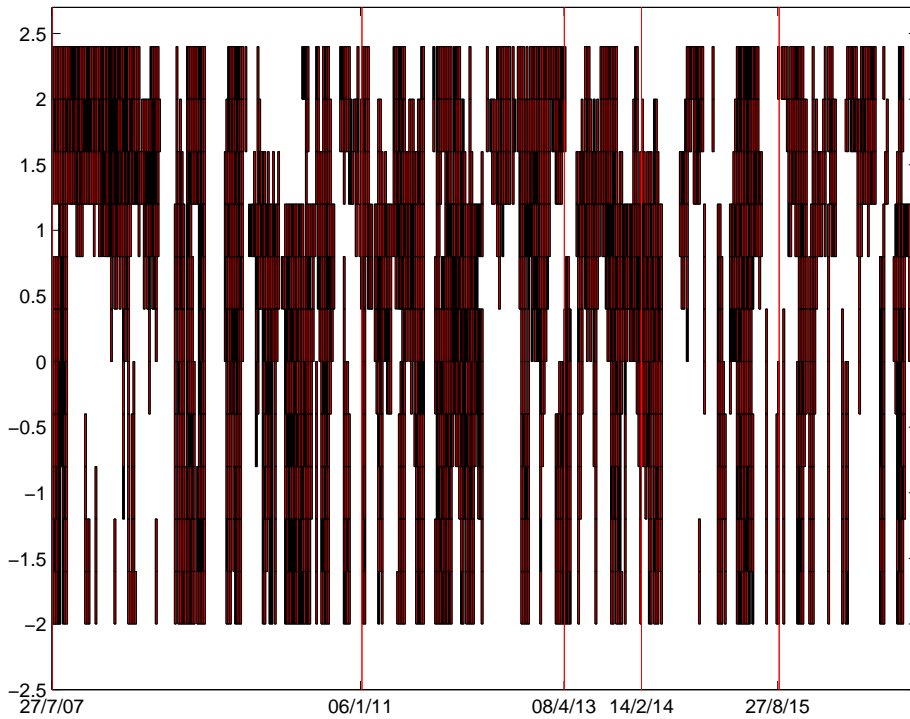
Figure 28: Forecast on the 5 days following a Bm time windows of length 75. The red squares at position (β_1, t) evidence that the forecast of the 5 days following a Bm time window of length 75, starting at time $t-1$ and characterized by the same parameter β_1 is better than the fBm one with H proper of the window starting at $t+5$, with the same β_1, and same length. Table 5 sums up the percentages of prevalence
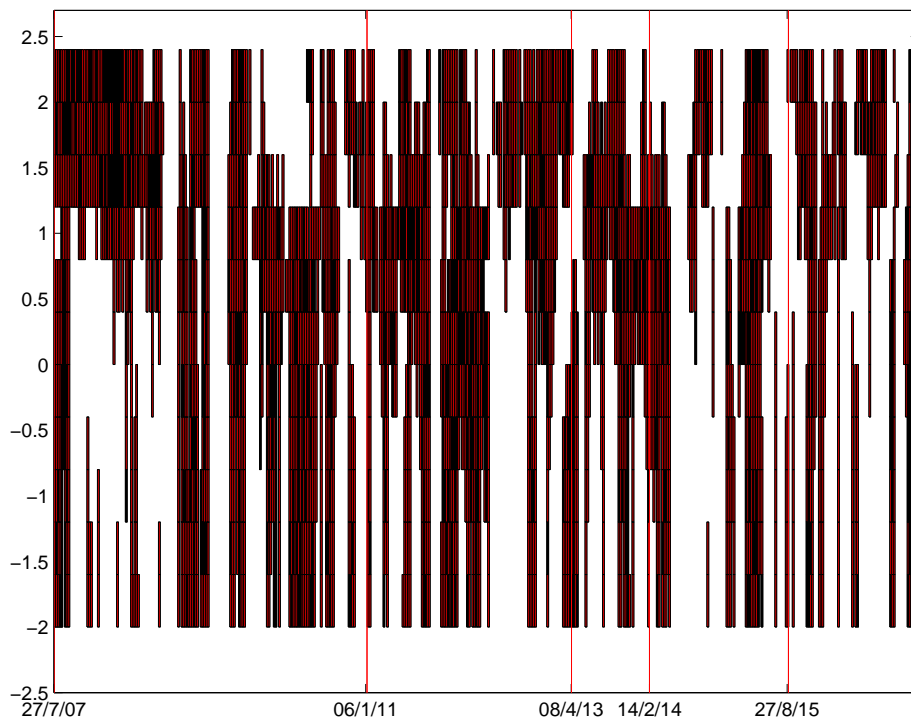
Figure 29: Forecast on the 5 days following a Bm time windows of length 100. The red squares at position (β_1, t) evidence that the forecast of the next 5 data based on a Bm assumption on the time window of length 100, starting at time t and characterized by the same parameter β_1 is better than the fBm one with H proper of the window starting at $t + 5$, with the same β_1, and same length. Table 5 sums up the percentages of prevalence.

48
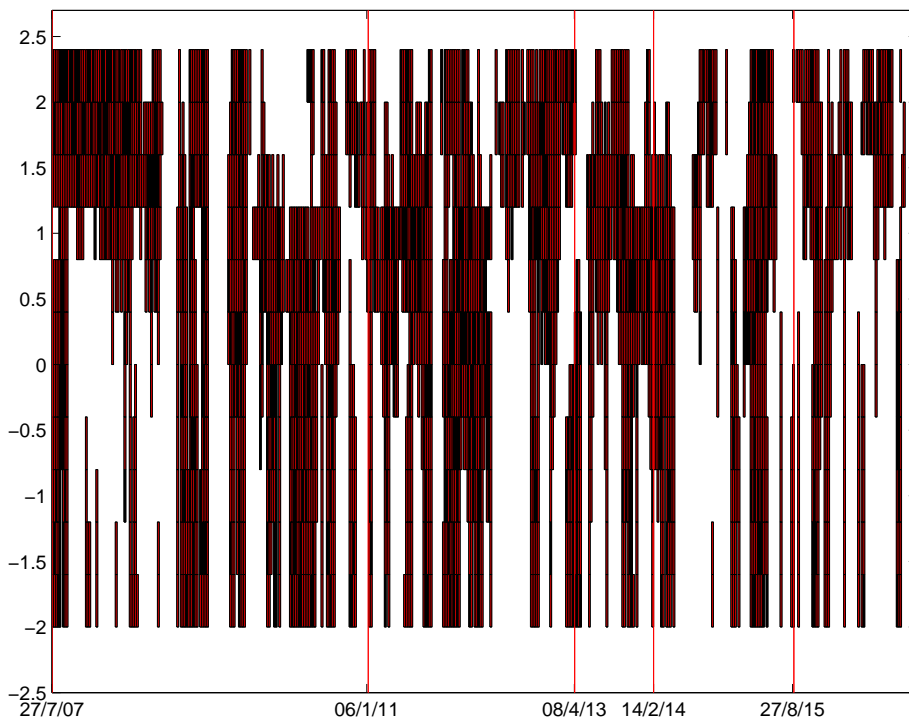
Figure 30: Forecast on the 5 days following a Bm time windows of length 125. The red squares at position (β_1, t) evidence that the forecast of the 5 days following a Bm time window of length 125, starting at time t and characterized by the same parameter β_1 is better than the fBm one with H proper of the window starting at $t+5$, with the same β_1, and same length. Table 5 sums up the percentages of prevalence.
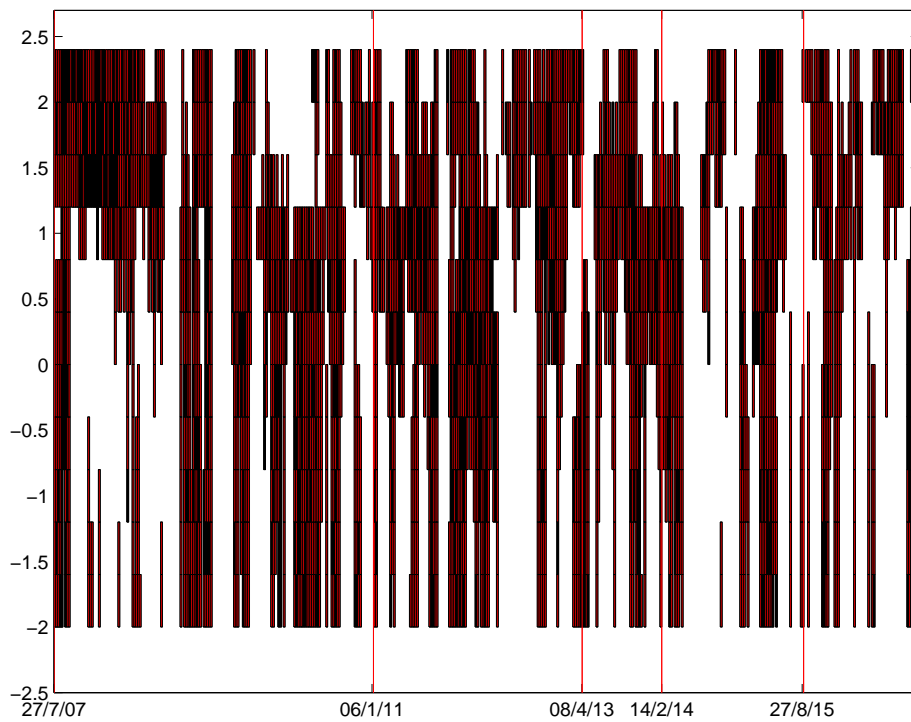
Figure 31: Forecast on the 5 days following a Bm time windows of length 150. The red squares at position (β_1, t) evidence that the forecast of the 5 days following a Bm time window of length 150, starting at time t and characterized by the same parameter β_1 is better than the fBm one with H proper of the window starting at $t + 5$, with the same β_1, and same length. Table 5 sums up the percentages of prevalence.
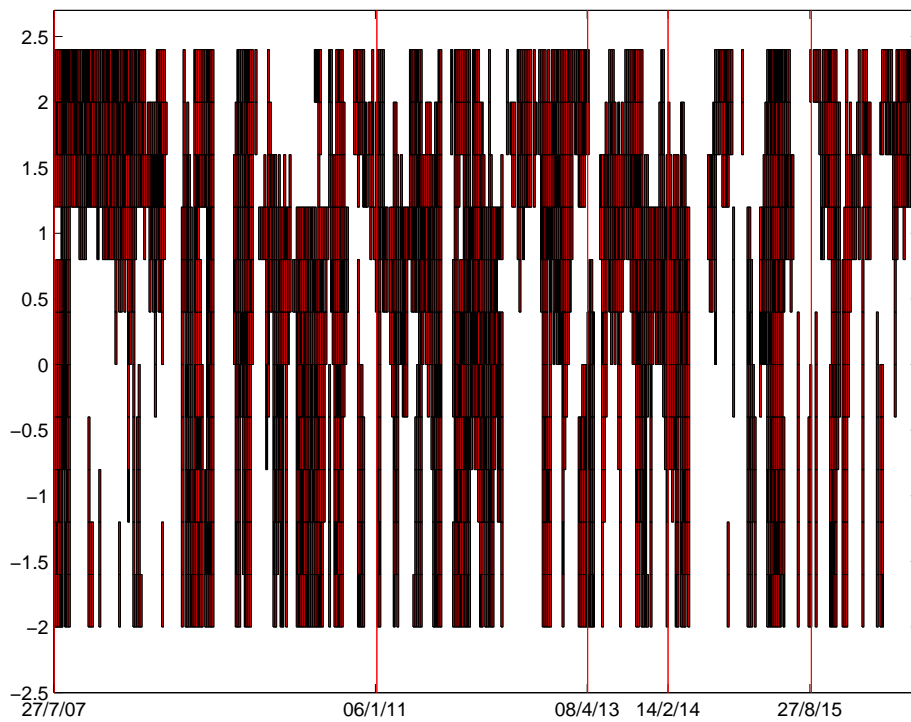
Figure 32: Forecast on the 5 days following a Bm time windows of length 175. The red squares at position (β_1, t) evidence that the forecast of the 5 days following a Bm time window of length 175, starting at time t and characterized by the same parameter β_1) is better than the fBm one with H proper of the window starting at $t + 5$, with the same β_1, and same length. Table 5 sums up the percentages of prevalence
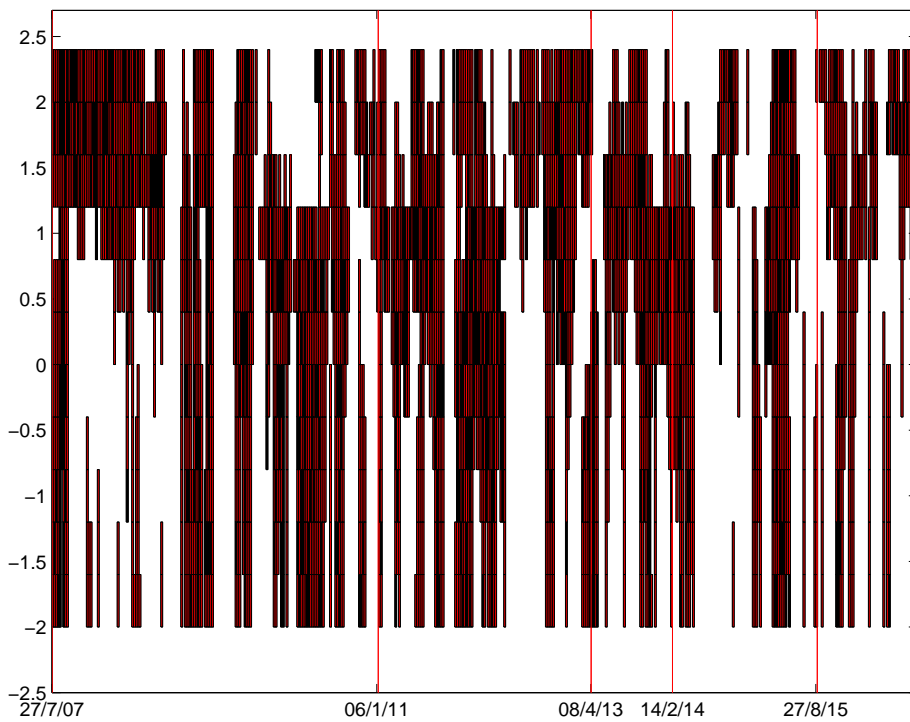
Figure 33: Forecast on the 5 days following a Bm time windows of length 200. The red squares at position (β_1, t) evidence that the forecast of the 5 days following a Bm time window of length 200, starting at time t and characterized by the same parameter β_1 is better than the fBm one with H proper of the window starting at $t+5$, with the same β_1, and same length. Table 5 sums up the percentages of prevalence.
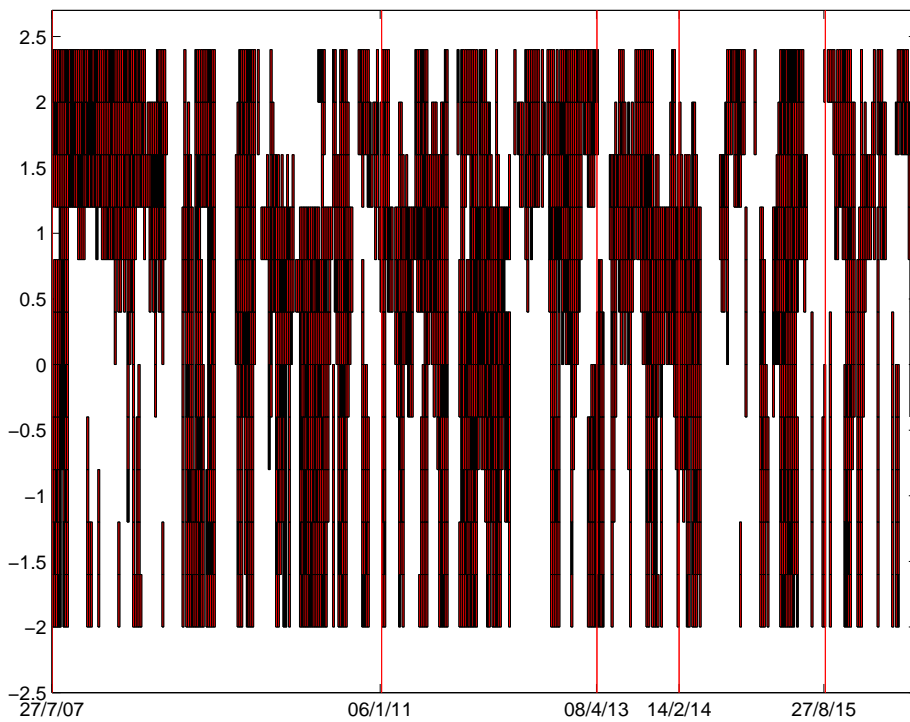
Figure 34: Forecast on the 5 days following a Bm time windows of length 225. The red squares at position (β_1, t) evidence that the forecast of the 5 days following a Bm time window of length 225, starting at time t and characterized by the same parameter β_1 is better than the fBm one with H proper of the window starting at $t+5$, with the same β_1, and same length. Table 5 sums up the percentages of prevalence.
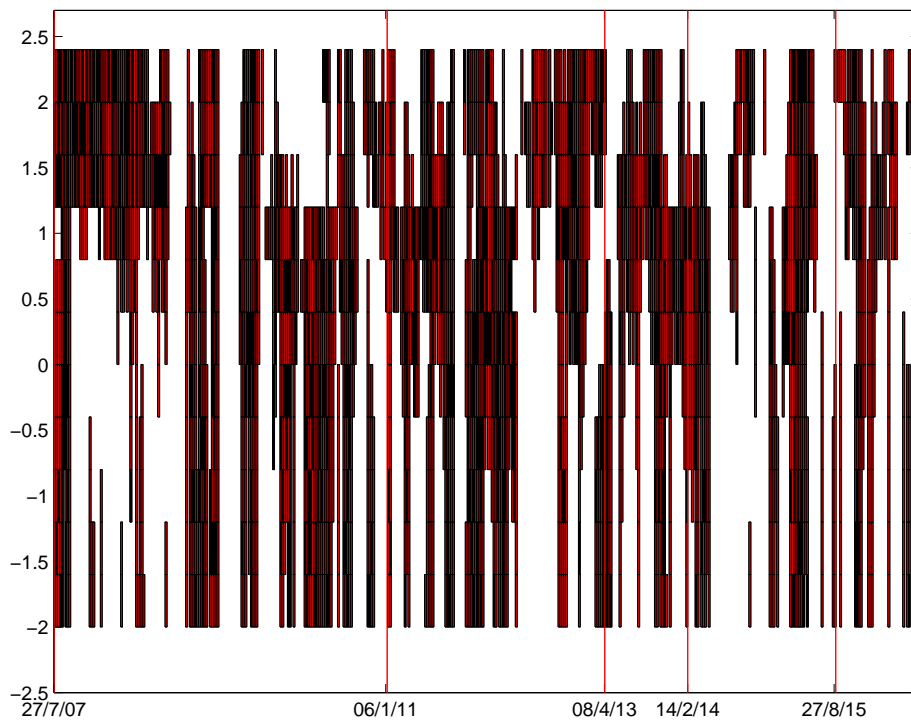
Figure 35: Forecast on the 5 days following a Bm time windows of length 250. The red squares at position (β_1, t) evidence that the forecast of the 5 days following a Bm time window of length 250, starting at time t and characterized by the same parameter β_1 is better than the fBm one with H proper of the window starting at $t+5$, with the same β_1, and same length. Table 5 sums up the percentages of prevalence.